

Trinity University

Digital Commons @ Trinity

Engineering Senior Design Reports

Engineering Science Department

4-15-2010

Design Review Report: Zero G Design Group

Dylan Brandt
Trinity University

Peter Garatoni
Trinity University

Sara Gerloff
Trinity University

Sawan Vaidya
Trinity University

Follow this and additional works at: https://digitalcommons.trinity.edu/engine_designreports

Repository Citation

Brandt, Dylan; Garatoni, Peter; Gerloff, Sara; and Vaidya, Sawan, "Design Review Report: Zero G Design Group" (2010). *Engineering Senior Design Reports*. 28.
https://digitalcommons.trinity.edu/engine_designreports/28

This Restricted Campus Only is brought to you for free and open access by the Engineering Science Department at Digital Commons @ Trinity. It has been accepted for inclusion in Engineering Senior Design Reports by an authorized administrator of Digital Commons @ Trinity. For more information, please contact jcostanz@trinity.edu.

TRINITY UNIVERSITY

Design Review Report

Senior Engineering Design

4/15/2010



Zero G Design Group

Dylan Brandt, Peter Garatoni, Sara Gerloff, Sawan Vaidya

Dr. Farzan Aminian, Dr. Jack Leifer, Advisors

? The purpose of this report is to describe the design, construction, and testing of an apparatus capable of testing and recording the deployment of thin film shells in a microgravity environment. The group has designed a prototype and ideal model to test a deceleration system that, in full scale, would provide sufficient deceleration without harming the testing apparatus. This project does not involve dropping the constructed apparatus and equipment. A counter weight chain and pulley system was chosen as the deceleration prototype for testing. Issues with budget and time constraints have limited aspects originally planned for completion in this phase of the project. Budgetary issues have restricted mounting of the electrical components within the fabricated apparatus and purchasing housing for the enclosure. Data from the prototype tests from the counterweight deceleration were collected and compared to an ideal model. Analysis of results determined that a counterweight system is sufficient for decelerating the load, but modifications need to be made to the model to accurately predict its behavior. Despite issues integrating the full system with the Efika, the automation timing sequence and video recording drivers have been successfully written and tested. In the face of obstacles and delays, the project is taking shape and the group feels confident with its direction and design.

Executive Summary

The purpose of this project is to design an apparatus capable of testing the deployment of thin film shells in a microgravity environment. Our project sponsor, Mevicon, of Sunnyvale, California, manufactures precision thin film material based shells for various space applications including RF apertures on satellites. The shells are *roll stowed* for launch and lift to orbit and are deployed in zero gravity. Mevicon wishes to quantitatively and qualitatively test, analyze and document the deployment behavior of the shells as they deploy in a zero gravity environment.

The most economically feasible option for simulating zero gravity is a drop test. From that conclusion, the project has proceeded forward toward designing and implementing an apparatus for integration with a drop test. Because of budget and time constraints, the goal of this project for the 2009-2010 school year is to design, construct, and test only an apparatus for testing of the shell deployment for a drop test that will be fully implemented in future work. Additionally, the group has designed a proof of concept prototype and ideal model to test a deceleration system that, in full scale, would provide the amount of free fall and relatively gentle deceleration following the free-fall period to stop the testing apparatus without harming it. These two goals are separate. The group is not going to integrate the apparatus with a drop test. The apparatus is designed to be capable of integration with a drop test, but it will be the goal of a future project to conduct a full scale drop test and collect microgravity data.

The test apparatus is constructed from extruded aluminum structural members. A finite element analysis software was used to verify structural integrity, however it failed to provide useful data. If future analysis suggests the present design will be unable to sustain the forces of

deceleration, recommendations of additional Bosch pieces for strengthening the beams have been selected.

The drop test and deceleration system design includes a prediction model for the drop and deceleration including velocity, drop time, and force required to stop the test apparatus. A scaled prototype with dummy weights representing the test apparatus has been constructed to verify the accuracy of the prediction model. Tests were run using the scaled prototype for different dummy weights, counterweights, and drop heights and recorded. These recordings allowed for video analysis in MATLAB resulting in quantitative data of the prototype drop tests. This data are graphed and directly compared to the results output from the model for each test.

In order to achieve a professional design that achieves the project objectives, an electronic automation system is implemented. The original design objectives state that the system be drop test ready by the end of Phase I. However, due to both technical and budgetary requirements, this was unobtainable. However, the final Phase I design includes all electronics necessary to trigger, deploy, and record the experiment, including USB2.0 CMOS cameras and a GPIO controlled by a desktop PC.

Unfortunately, there remain several loose ends from Phase I that will spill over into Phase II of the project in the upcoming year. Numerical simulations need to be done to verify the strength of the test apparatus, the electrical components in the automation system need to be mounted, and housing needs to be purchased and installed to fully enclose the structure. Finally the automation system must be made drop test ready by eliminating the desktop computer one way or another.

Table of Contents

Executive Summary	ii
Table of Figures	vi
Table of Tables	vii
1 Introduction	1
2 Design Overview	4
2.1 <i>Decelerating Mechanism</i>	4
2.1.1 Design Concept for Fully Functional System	4
2.1.2 Modeling Deceleration	6
2.1.3 Model Interpretation.....	9
2.1.4 Deceleration Prototype Parts	10
2.2 <i>Case Structure and Layout</i>	11
2.3 <i>Original Design Objectives</i>	11
2.4 <i>Final Design</i>	12
2.4.1 Construction / Mounts	15
2.5 <i>Automation System</i>	20
2.5.1 Original Design Objectives.....	21
2.5.2 Issues Preventing Full Implementation	23
2.5.3 Phase I Final Design	25
3 Methods	28
3.1 <i>Deceleration System</i>	28
3.2 <i>Apparatus System – ProMechanica</i>	28
4 Results	31
4.1 <i>Deceleration System</i>	31
4.2 <i>Apparatus System – Simple Model</i>	36
5 Conclusions and Recommendations.....	38
5.1 <i>Deceleration Model and Prototype</i>	38
5.2 <i>Recommendations for Measuring Techniques</i>	39
5.3 <i>Apparatus System</i>	41
5.4 <i>Automation System</i>	43

6	Bibliography.....	47
A	Drawings.....	A-1
B	Plots.....	B-1
C	Calculations	C-1
C.1	<i>Freefall Calculations (Without chain).....</i>	C-1
C.2	<i>General Deceleration Calculations</i>	C-2
C.3	<i>Exact Solution of Deceleration Model</i>	C-3
D	Deceleration System Data Collection	D-1
E	Specifications.....	E-1
E.1	<i>Efika MX Specifications^[10]</i>	E-1
E.2	<i>Efika 5200B Specifications.....</i>	E-2
E.3	<i>Camera Specifications^[7]</i>	E-3
E.4	<i>Lens Specifications^[7]</i>	E-4
E.5	<i>Circuit Board Relay Specifications</i>	E-5
E.6	<i>Darlington Array Specifications.....</i>	E-6
E.7	<i>USB - I2C/SPI/GPIO Adapter - U2C-12 Specifications</i>	E-7
F	West Brook Metals Information Sheet.....	F-1
G	Test Matrix.....	G-1
H	Bill of Materials and Vendor List	H-1
I	Schedule	I-1
J	Budget	J-1

Table of Figures

Figure 1: Prototype deceleration and measurement schematic.....	7
Figure 2: A general velocity vs. time curve showing freefall and deceleration.....	10
Figure 3: Bench Plate and Mounting Hardware for 20 Inch Shell.....	13
Figure 4: Original Design of Apparatus with Mounting Hardware and Cameras.....	14
Figure 5: Final Design of Apparatus with Mounting Hardware and Cameras.....	15
Figure 6: Camera 1 and 2 Mount Locations	17
Figure 7: Camera 2 Mount Location and Field of View	17
Figure 8: Multi Angle Fastener with Camera.....	18
Figure 9: Apparatus with Mounts.....	20
Figure 10: Sequence of Events.....	21
Figure 11: Board Level (left) and Enclosed (right) Camera Versions ^[7]	22
Figure 12: Driver Circuit.....	27
Figure 13: Simplified Apparatus Pro E Drawing.....	30
Figure 14: Plot of 15 lb Object in Freefall, Actual Results vs. Model	31
Figure 15: Plot of 5 lb Object in Freefall, Actual Results vs. Model	32
Figure 16: Plot of 10 lb Object in Deceleration after 3 Feet of Freefall, Actual Results vs. Model.....	34
Figure 17: Plot of 10 lb Object in Deceleration after 9 Feet of Freefall, Actual Results vs. Model.....	35
Figure 18: Plot of 10 lb Object in Deceleration after 9 Feet of Freefall, Actual Results vs. Model.....	36
Figure 19: Right Angle Gusset ^[3]	41
Figure A-1: Corner Cube ^[3]	A-1
Figure A-2: Inside-to-Inside Gusset ^[3]	A-1
Figure A-3: Multi Angle Fastener ^[3]	A-2
Figure A-4: Schematic of Counter Weight Decelerating System.....	A-3
Figure B-1: Acceleration due to gravity felt vs. Time for different drag coefficients.....	B-1
Figure B-2: Drop distance vs. Time for varying drag coefficients	B-1
Figure B-3: Velocity of falling object vs. Time for varying drag coefficients (Cd is drag coefficient).....	B-2
Figure B-4: Number of Gs required to decelerate a 100kg mass that was dropped from 120 feet given that that deceleration starts from at a height of 'h' feet and only 'h*f' feet is available for deceleration	B-2
Figure D-1: Plot of actual distance versus pixels distance used to derive a conversion factor.	D-3
Figure E-1: Efika MX Microcomputer.....	E-1
Figure E-2: Efika5200B Microcomputer.....	E-2

Table of Tables

<i>Table F-1: Housing Size and Cost Estimate.....</i>	<i>F-1</i>
<i>Table H-1: Bill of Materials and Vendor List</i>	<i>H-1</i>
<i>Table J-1: Project Income.....</i>	<i>J-1</i>
<i>Table J-2: Project Expenses.....</i>	<i>J-2</i>

1 Introduction

Mevicon, Inc., based in Sunnyvale, California produces various sizes of thin film shells used mainly for various applications in outer space. In this project, the apparatus will be designed around testing shell sizes with 12 inch and 20 inch diameters. These shells can be used as optical apertures for orbiting telescopes and can also be implemented into deployable orbiting radio frequency apertures. While bringing the shells in to outer space via spacecraft, they must each be rolled up very tightly in a cylinder while being held in place by the deployment hardware. Once a shell has arrived at its destination in the zero gravity environment, deployment hardware is activated, allowing the shell to break free from the deployment hardware, unroll itself, and assume its original shape.

Previous testing was conducted by the University of Kentucky in conjunction with NASA to test the shell deployment on a NASA zero-gravity simulating airplane.^[1] Also known as the “vomit-comet,” this airplane flies in repeated parabolic trajectories and affects short periods of microgravity on passengers and onboard equipment in the unpowered portion of the flight (essentially zero-g). This testing method provides the microgravity environment required, but is extremely expensive.

Due to the high cost and very limited access of testing experiments in zero gravity conditions, it is extremely difficult for Mevicon, Inc. to test the deployment behavior of the thin film shells that they produce. Testing and analyzing the deployment behavior of these shells is very important since they will be used in outer space along with many other major pieces of equipment. For instance, the analysis of the deployment behavior may reveal that there is a lot of chaotic and random motion involved with the shells as they unroll and return to their original

shape in zero gravity. If this were to actually happen, the shells would probably not be used for any space applications until the deployment process was reformed so that they can be released in a very uniform fashion in zero gravity. For this reason, Mevicon proposed a senior design project to the Trinity Engineering Science Department to design a method for recording the shell deployment in a ground based microgravity environment. The initial proposal called for a one year project to design and implement a full drop test. In the fall semester this goal was determined to be too ambitious for the given timeframe and budget. Subsequently, the project was divided into two phases. Phase I would design the test apparatus and a prototype deceleration system and Phase II would implement this design in a full scaled drop test (Note: all references in this report to the "project" or "design" are regarding Phase I only).

The purpose this project (Phase I) is to design an apparatus that can record the deployment behavior of precision thin film material based shells intended for use in a zero gravity environment, and construct a proof of concept prototype consisting of a scaled down drop test, incorporating a dummy load, and decelerating system. The apparatus should be capable of deploying a sample of the thin-film material in a free fall drop test, and record the deployment behavior through video in such a way that can be analyzed using existing MatLAB scripts. The apparatus should allow for repeated testing and be durable enough as to not damage any experimental equipment contained inside when dropped. This design will not include a drop test involving the deployment of the thin film test article.

Although the deployment behavior in zero gravity will not be recorded or analyzed this year, this project provides the footing for a potential senior design group in the future. The two phases allows for a larger timeframe and budget to ensure completion and functionality. In Phase II, a drag shield to reduce drag forces on the existing apparatus and achieve microgravity will be

designed and implemented. In addition, Phase II will consider proof of concept established in Phase I and design and implement a drop test with reasonable deceleration, as to not damage the test apparatus or equipment inside while still achieving required time for freefall. Finally, the resulting video will be analyzed using the existing MatLAB scripts and presented to Mevicon.

2 Design Overview

The completed design consists of three subsystems: a deceleration system to ensure the safety of the apparatus as well as the safety of the environment and people involved, an apparatus for mounting and deploying the shell, and a video recording system to record the deployment event during free fall. The team intends to present a proof of concept of the deceleration mechanism. The stopping point for this phase of the design is the completion of a working prototype of the decelerating mechanism and a drop test apparatus.

2.1 *Decelerating Mechanism*

From Figure B-3, a plot of velocity vs. time for the apparatus in freefall, it can be seen that a maximum velocity of near 20m/s can be attained during freefall in roughly 2 seconds. With only 10.2 g's of force, an object traveling at this velocity can be brought to rest in about 2 meters (approx. 6.5 feet) given that uniform deceleration is provided. The relationship between required number of g's and the available deceleration height can be seen from Figure B-4. In this case, a 100 kg object and a drop height of 120 feet (height of Murchison Tower) was considered. The height at which the object starts to decelerate is given on the abscissa and the acceleration (in g's) needed to decelerate to zero speed using only one-half of the height available from the point deceleration commences to the ground is provided on the ordinate.

2.1.1 Design Concept for Fully Functional System

In the completed design, two pulleys will be attached under a top platform and a rope will pass above them. The apparatus will be attached to one end of the rope and the counter weights will be attached to the other end. The drag shield, when implemented, rests on the apparatus as

shown in Figure A-4. Attaching the ropes to the drag shield instead of the apparatus can be considered since this would prevent the apparatus from getting the brunt of the decelerating force by distributing the concentrated tension force over a greater surface area (the bottom of the apparatus). Parallel guide wires that connect the top platform to the bottom platform can be used to ensure stability during the drop. The guide wires are for safety only and should not come into contact with the drag shield during the free fall stage so as to prevent friction. When released, the apparatus along with the drag shield fall freely, until the rope attached to the drag shield becomes taut. Counter masses are loaded on to the other end of the rope one at a time gradually increasing the counter force, minimizing the “jerk” (the rate of change of acceleration) that is acting on the apparatus. For safety, a soft cushion can be placed on the bottom platform. This design is an adaptation of an original counter weight deceleration solution proposed by Scott A. Leva.^[2]

Before the required time in freefall is achieved, the rope connecting the counter weights to the apparatus is slack. Therefore the apparatus is in freefall until the rope is taut. When the rope becomes taut large jerking forces result from increasing mass over a short period of time. Seen in Equation (C-8), the rate of change of momentum ($m_i \cdot v$) with respect to time directly affects the tension in the cable. To avoid the problem of strong jerking forces, a system of continuously increasing counter masses was proposed as a deceleration prototype in Phase I.

The purpose of the deceleration prototype in Phase I is to determine the rate at which the counter mass needs to be increased to achieve a desired deceleration. The prototype system utilizes a heavy, metallic chain. Through testing, the group will determine the optimum total counter mass parameters. If a heavy enough chain is not available, the effects of the chain can be approximated in Phase II by loading a series of weights. The experiments will also reveal the exact nature of forces that are involved in the system.

2.1.2 Modeling Deceleration

Assumptions that were made in order to derive a model for deceleration using the chain counterweight are as follows:

1. The tension in the rope connecting the apparatus to the counterweight chain is constant through the pulleys. This is not the case when there is friction between the rope and the pulleys. In other words, it was assumed that friction is negligible.
2. The moment of inertia of the pulleys is negligible, which means that no energy is required to bring the pulleys in motion and that pulleys do not exert a force on the ropes preventing the object from stopping.
3. The rings in the chain are of infinitesimal size and thus the rate of change of mass of the chain when it is being lifted up is continuous.
4. The friction in the chain is negligible and the rings of the chain rubbing against each other do not dissipate energy.
5. Air resistance for chain and cable is negligible.
6. The tugging on the rope due to horizontal motion of the load is negligible. In other words, the load does not swing during drop.

In an ideal case, a simple free body diagram around the apparatus and the chain help to obtain the differential equation for governing deceleration. Figure 1 shows the experimental prototype.

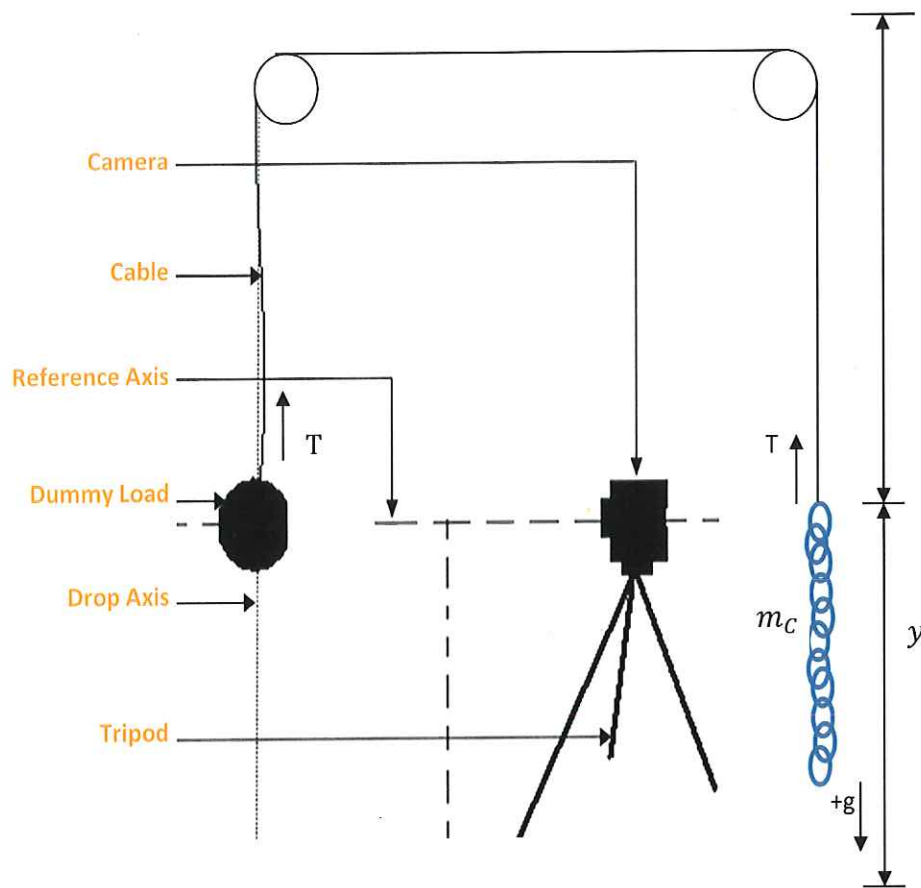


Figure 1: Prototype deceleration and measurement schematic

$$m_A g - T = m_A a_A \quad (1)$$

$$T - m_c g = \frac{dm_c v_c}{dt} \quad (2)$$

Adding the equations and expanding the differential term by use of the product rule, the ~~following equation~~ ⁽³⁾ is obtained

$$m_A g - m_c g = m_A a_A + m_c \frac{dv_c}{dt} + v_c \frac{dm_c}{dt} \quad (3)$$

The mass of the chain is the product of its mass per unit length (ρ) times its length. In addition to this substitution, the mass of the apparatus is substituted by the product of ρ and equivalent chain length of mass (y_A). The equivalent chain length of mass is a constant and helps to simplify the equation as follows:

Let, $m_C = \rho y$ and $m_A = \rho y_A$

$$\rho y_A g - \rho y g = \rho y_A a_A + \rho y \frac{dv_C}{dt} + v_C \frac{d\rho y_C}{dt} \quad (4)$$

The density, ρ can now be cancelled out from (4) after the substitution.

The velocity of the counterweight is half the velocity of the apparatus itself because the center of gravity of the chain does not move at the same speed as the tip of the chain. The tip of the chain however, moves at the same speed as the apparatus. The following substitutions are made:

$$v_C = -\frac{1}{2} v_A \text{ and } \frac{dy_C}{dt} = 2v_C = -v_A, \text{ thus}$$

$$y_A g - y g = y_A a_A + \frac{1}{2} y \frac{dv_A}{dt} + \frac{1}{2} (v_A)^2 \quad (5)$$

With a little rearrangement, and setting $\frac{dv_A}{dt}$ to a_A , the following differential equation was obtained:

$$a_A \left(\frac{y}{2} + y_A \right) + \frac{1}{2} (v_A)^2 + g(y - y_A) = 0 \quad (6)$$

The resulting model is a second order nonlinear differential equation. Computation of the exact solution is a tedious process. Hence Euler's approximation was employed for a numerical solution of the differential equation. An exact solution was derived however not used because, the solution turned out to be more computationally demanding than a numerical solution and still not more accurate. The exact solution derivation is listed in Appendix C.3. Notice the integrals

involved in Equation (C-28) . The computational time taken for the computer to solve these integrals made the exact solution more tedious to process than the numerical solution using Euler's approximation.

Assuming $a_A = \frac{v_A(t+\Delta t)-v_A(t)}{\Delta t}$ and $v_A = \frac{y(t+\Delta t)-y(t)}{\Delta t}$, combined with the differential equation above, the following numerical equations can be derived:

$$y(t + \Delta t) = v_A(t)\Delta t + y(t) \quad (7)$$

$$v(t + \Delta t) = \frac{-g(y - y_A) - \frac{1}{2}(v_A(t))^2}{\left(\frac{y}{2} + y_A\right)}\Delta t + v_A(t) \quad (8)$$

MATLab or Excel can now be used to generate a table of values for these equations, given an initial displacement ($y(0)$) and an initial velocity ($v_A(0)$).

2.1.3 Model Interpretation

In Figure 2, the first portion of the graph represents the object in freefall and the second portion represents the effect of the counterweight. When the rope becomes taut, the counterweight comes into play and the rate of change of velocity decreases. The object eventually slows down and stops. The rate of decrease of speed seems lower than the rate of increase of speed. The distance required to stop the falling object has been found to be greater than the distance required to bring it to its maximum velocity during freefall.

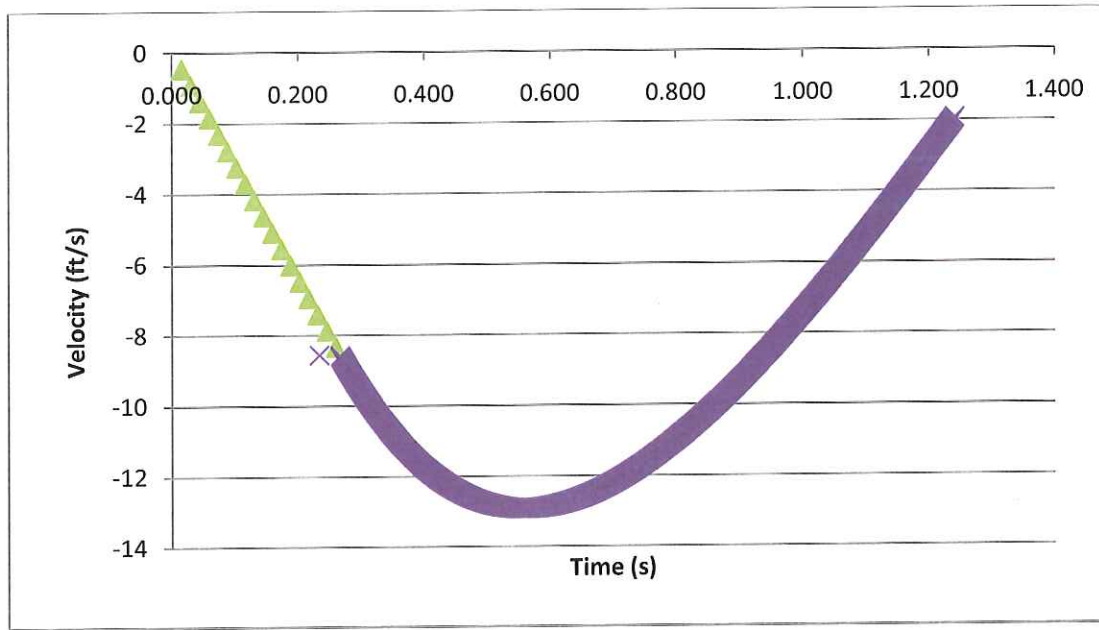


Figure 2: A general velocity vs. time curve showing freefall and deceleration

2.1.4 Deceleration Prototype Parts

The parts used for prototype deceleration system were purchased from Grainger Industrial Supply. Calculations based on the model showed that the maximum tension (T_{\max}) in the rope would be 38.3 lbs. Since the rope passes above two pulleys, the equal tension forces are perpendicular to each other. The maximum total force in the pulley was therefore assumed to be $T_{\max}\sqrt{2}$ which is equal to 54.3 lbs. Pulleys obtained from Grainger can withstand a forces up to 800 lbs, which is well above the maximum tension force needed for the prototype. Galvanized cables that were used in the design have a maximum tension specification of 1400 lbs. A chain was purchased for counterweight, which weighed 2.22lb/ft. Since the chain could be folded, its weight per unit length could be multiplied. The chain was folded up to 7 times in the experiments making the maximum weight per unit length equal to 15.54 lb/ft. An eye bolt release mechanism

was devised which consisted of a metallic loop and a bolt. When the bolt was pulled out of the loop the object was free to fall.

2.2 Case Structure and Layout

As stated above, a case is required to mount the deployment hardware for the shells, as well as the cameras and related electronic equipment so as to withstand the effects of the decelerating force. In researching materials for this apparatus it was chosen to use a company that produces prefabricated aluminum framing. A prefabricated frame provides the precision and professionalism the apparatus requires. The apparatus itself is constrained based on the following requirements. The deployment hardware will be attached to the apparatus frame and the apparatus dimensions should not restrict deployment of shells of up to 20 inches. The test apparatus must allow for secure mounting of the cameras, the Efika microcomputer, a power supply, lights, and related electrical equipment. It must ensure the shell deployment behavior is unaffected by dynamic air flows and there is uniform lighting for proper recording of the deployment. The most important function of the apparatus however, is to withstand repeated drops from the specified drop height, while keeping all electrical components held within completely intact and unaffected.

2.3 Original Design Objectives

Based on cost and previous designs, Bosch Rexroth Corporation^[3] was chosen as the manufacturer for the prefabricated frame. The deployment hardware held within is comprised of the mounting hardware and a solenoid firing mechanism, provided by Mevicon, and requires a bench plate with predrilled ¼"-20 holes to install. Mevicon purchased and supplied a 36"x 4" bench plate for the project.^[4] The original size of the apparatus was a cube with length, width,

and height 36 inches (914 mm). The bench plate chosen required the minimum length of the apparatus to be 36 inches for proper mounting. The width and height were chosen to be 36 inches as well to allow room for the other electronics, and to allow a minimum object distance for a standard video camera to capture the full deployment of the shell. This initial sizing of the apparatus allows for multiple cameras to be used, as well as plenty of space to allow mounting any other electrical equipment. The dimensions for the length and height of the frame were reevaluated for the specific cameras and lenses chosen and to reduce cost of materials. The resulting smaller surface area will also reduce the size of the drag shield and consequently the drag force.

2.4 Final Design

As stated above, the apparatus frame was reassessed based on the minimum object distances required for the Mightex cameras and lenses, to reduce cost of materials, and to allow entry into the Murchison Tower if it is later chosen as the drop site. The entry door to the tower is not large enough for the original dimensions of the apparatus and cannot be altered without jeopardizing the tower's structural integrity. For the predrilled holes of the bench plate to align exactly with the center of the Bosch strut for mounting, the four lengths of the strut are calculated to be 849mm long. Bosch is a company that works internationally and only deals with SI units. With the two corner cubes attached, each 40mm long, the total length is 889mm. Based on the minimum object distance for the Mightex cameras and lens attachments of 0.1 m, as can be seen on the data sheet in Appendix E.4, the height and width of the apparatus strut is calculated to be 635mm each. With two corner cubes attached, the height and width are 715mm. This allows for a full image to be captured of the 20 inch shell deployment, while keeping the height and width of the apparatus to a minimum.

As stated above, Mevicon has provided the bench plate, deployment hardware, and shells to be tested for this design. A Pro-E sketch of this hardware mounted to the bench plate can be seen below in Figure 3.

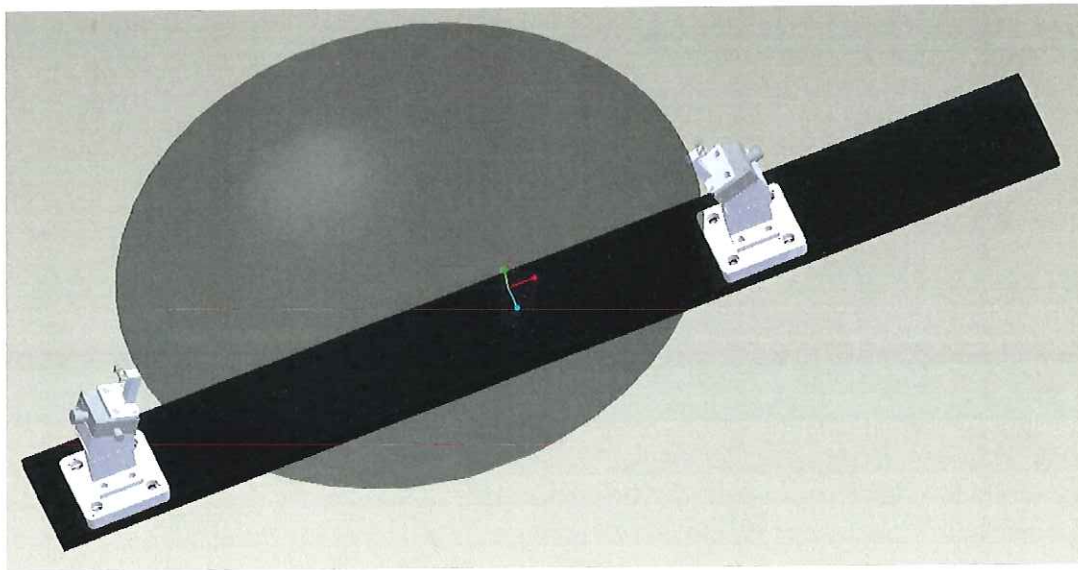


Figure 3: Bench Plate and Mounting Hardware for 20 Inch Shell

The aluminum frame apparatus from Bosch allowed for easy construction and a wide range of accompaniments for mounting additional pieces. The apparatus itself consists of 14 40x40 mm cross section beams connected in a cube with 2 extra beams for mounting the two cameras. The beams are joined at the corners by what Bosch calls corner cubes, which allow easy and sturdy assembly. The two additional beams are connected using four inside-to-inside gussets. Close up Pro-E drawings of the corner cubes and inside-to-inside gussets can be seen as Figure A- and Figure A-2 in Appendix A.

Bosch sells the aluminum strut pieces in lengths of 6 meters. With resizing of the apparatus, only two 6 meter lengths were required for this design. Instead of ordering the full 6

meter pieces and cutting them ourselves, it was decided to order pre-cut lengths. This minimized cost of the material, cost of shipping, and did not result in extra, unused pieces. An original design was drawn in Pro-E to visualize the above stated issues, with the mounting hardware and cameras in place, and can be seen ~~below~~ in Figure 4.

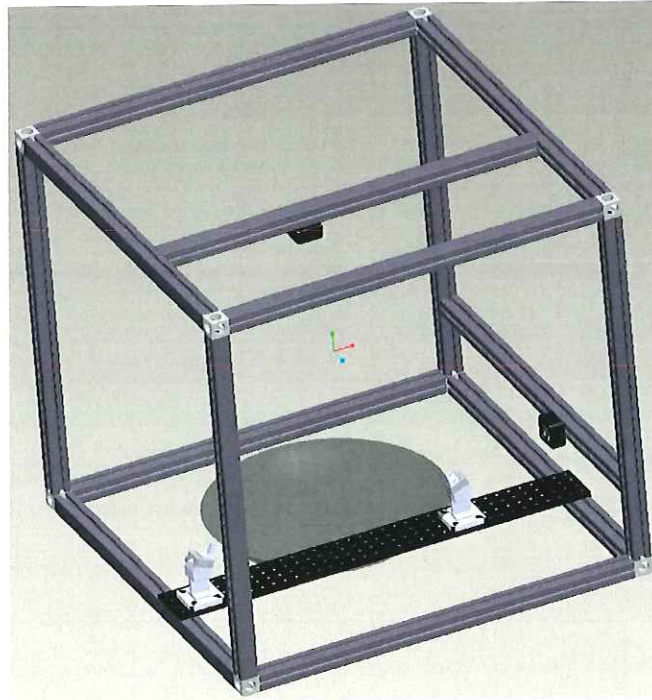
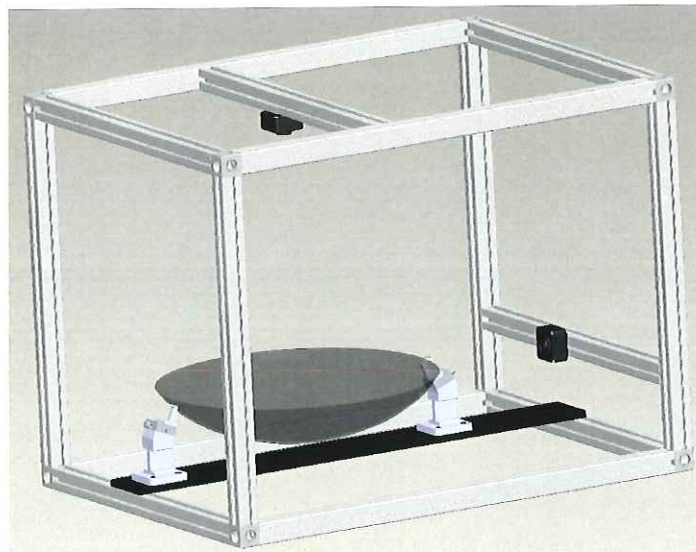


Figure 4: Original Design of Apparatus with Mounting Hardware and Cameras

Figure 4 clearly displays the basic design of the apparatus with bench plate, mounting hardware, a 20 inch shell, and two cameras mounted. As can be seen above, sizing the apparatus as a 36"x36"x36" cube creates plenty of space for future electronic placement. The final design of this apparatus will include the deployment hardware, lighting, video recording system (cameras and Efika MX micro-computer), release system and required power supply all securely mounted to the frame. The reevaluated dimensions of the frame were redrawn in Pro-E and can

be seen ~~below~~ in Figure 5. The final dimensions are 849x635x635mm. This figure does not contain the final mounting pieces for the cameras and additional materials needed for the video recording system, but is a good reference for comparing the reduction in size dimensions from the first design.



B4/After
a la
Rotenberg...
Same view/
scale.

Figure 5: Final Design of Apparatus with Mounting Hardware and Cameras

The size reduction is apparent when comparing the two above figures, as the overall volume of the box has reduced by 45%. Altering the width of the apparatus has allowed for the additional beams, used for camera supports, to reduce to 635mm from 914mm.

Cost/% reduction?

2.4.1 Construction / Mounts

Construction of the apparatus was completed in 4 hours using two members of the design team. Connecting the corner cubes to the strut required the purchase of a set of torx heads that were not on hand in the machine shop. Each corner cube required 3 screws to connect to the

screws?
screws?
etc?

strut. These screws required exceptional force as they threaded the aluminum as they were screwed in. Because of this, the screws were set into the strut pieces by themselves to produce a threading, then backed out, and then connected using the corner cubes. The inside-to-inside gussets must be set into the grooves of the respective pieces of strut before the corner cubes are attached, otherwise they cannot be used. Once completed, it was a simple task of attaching the bench plate to the strut using 4 T-Nuts and 4 ¼"-20 screws.

To record the deployment of the shells, two cameras from two separate vantage points are used. They can be seen rendered in black above in Figure 5. The MATLAB script, written by Mevicon, used to analyze the video of the shell deployment requires that the cameras be placed in the two locations shown. Camera 1 is placed directly above the center of the shell and camera 2 is mounted in line with the shell behind the mounting hardware. These two cameras provide the adequate frame of reference to fully document and analyze the deployment of the precision thin film material based shells. Figure 6 and Figure 7 below show a close up view of the camera mount locations. The cameras themselves and the respective video recording hardware are discussed in section 2.5.1 as a separate subsystem.

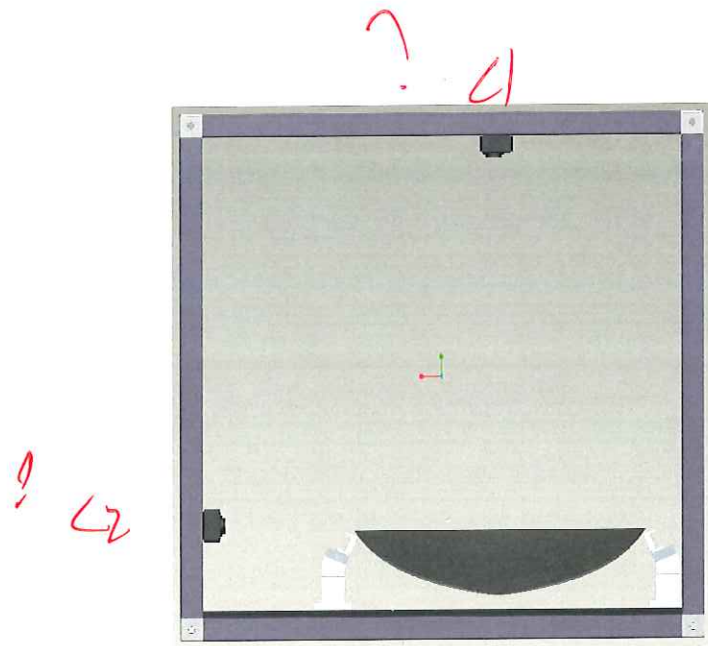


Figure 6: Camera 1 and 2 Mount Locations

*Doesn't match
fig?*

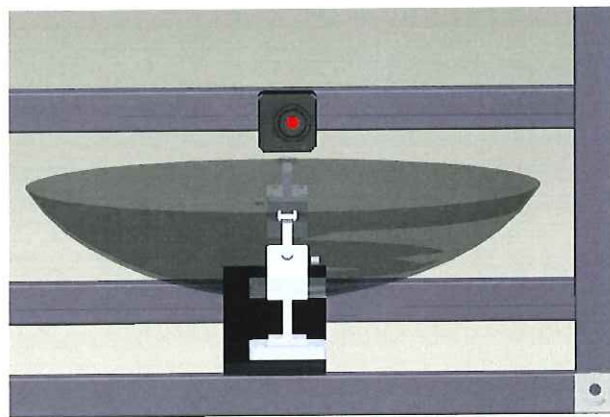


Figure 7: Camera 2 Mount Location and Field of View

Under

C1?

After reviewing optional mounts for the cameras, a multi angle fastener made by Bosch was chosen. The multi angle fastener can be seen as Figure A-3 in Appendix A. The fastener is connected directly to the supporting strut on one end and a 40x40mm piece of strut at the other. This 40x40mm piece of strut allows for a 1/4"-20 T-Bolt to connect the fastener and the threading

of the camera, holding it securely in position. The multi angle fastener is made to connect with the strut and allows for the cameras, with threading on the topside, to be mounted at a 90 degree angle from the strut, facing the shell. The multi angle fastener with camera mounted to the frame can be seen below in Figure 8.



Figure 8: Multi Angle Fastener with Camera

As stated above, one of the main design constraints of the apparatus is to ensure the shell deployment behavior is unabated by dynamic air flows. This, along with the need for uniform lighting for the cameras, requires that the apparatus be fully enclosed. Silicon encased LED strips made by Ozniium are chosen as light sources. These LED strips are easily mounted to the

Have been?

strut, and should allow for uniform lighting of the shells within the apparatus. There is also no threat of the LED lights being harmed during the deceleration of the apparatus.

Additional strut pieces and T-Nuts have been purchased to mount the Efika, batteries, and electrical components, including the driver circuit for the actuator and the GPIO that will be discussed later. Due to budgetary issues and time constraints, ~~a box~~ for mounting this equipment as well as pieces for enclosing the apparatus were not purchased and hence not connected to the apparatus. Components that have been purchased allow for mounting the cameras, bench plate, and mounting hardware only. Further explanation can be found in the conclusions and recommendations section of this paper.

It was decided to use one actuator for deploying the rolled up shells within the apparatus. Unlabeled
This actuator is connected directly to the bench plate using two ¼"-20 screws and bolts. Because the holes in the bench plate are pre-threaded, an electric drill was used to bore out the threading, allowing the screws to be placed securely mounting the actuator. The actuator is affixed to the bench plate at the approximate middle of the 12" shell, but can be moved to any location on the plate for use with any size shell up to 20". Threading has already been removed for affixing the actuator in the middle of a 20" shell. A photo of the apparatus with mounting hardware, cameras, and a 12" shell securely installed within can be seen below in Figure 9.

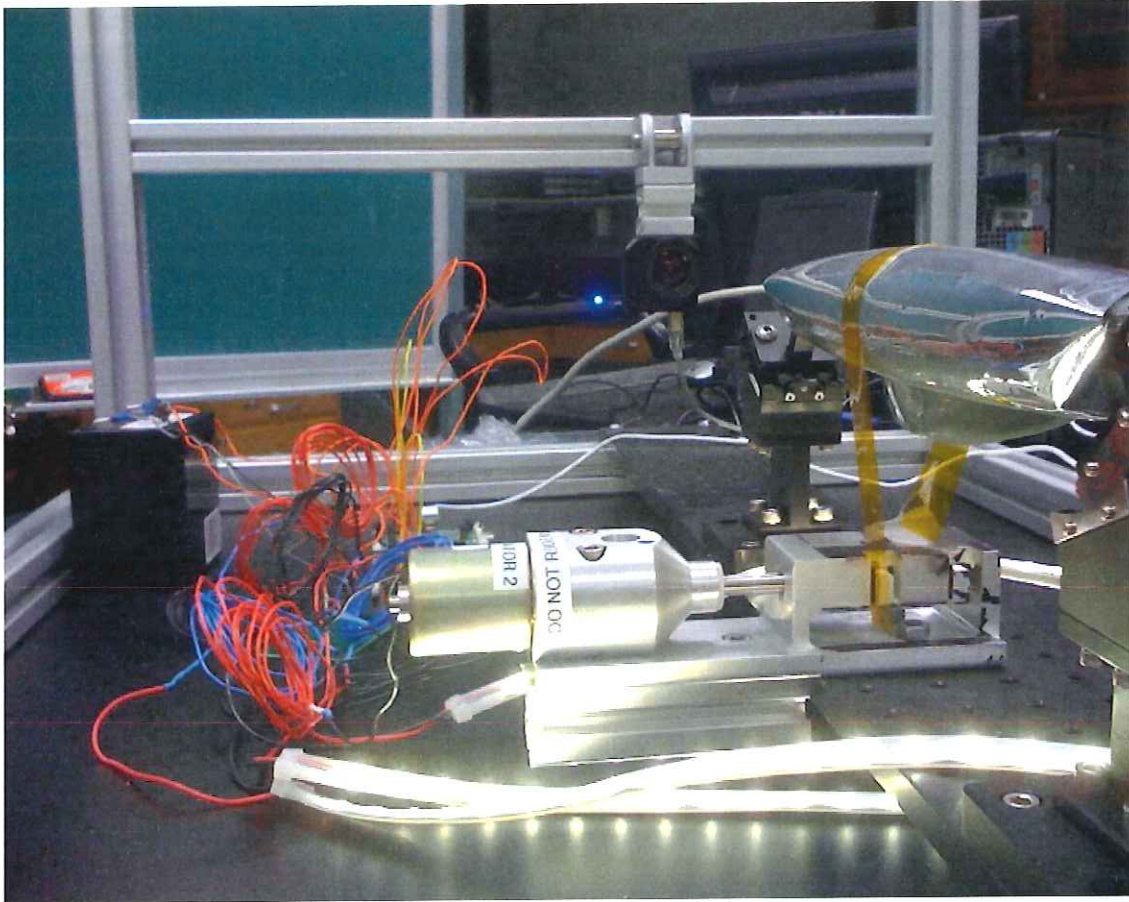


Figure 9: Apparatus with Mounts

2.5 Automation System

A successful drop test with useable video data depends on a sequence of events occurring in a short period of time, as explained below. A general time line of these events is shown in Figure 10.



Figure 10: Sequence of Events

Precise control of this event sequence is crucial to achieve the project objectives. The expected deployment time for a 20 inch shell is 1.5 seconds and the eventual drop site and deceleration system will allow for at least 1.5 seconds of freefall. Due to the need for precise control of the drop sequence, an automated electronic control system was selected. The control system includes a computer, cameras, and the I/O hardware required to detect the quick release mechanism and trigger the shell deployment.

2.5.1 Original Design Objectives

The components of the automation system, particularly the controlling computer and the cameras, must be robust and shock resistant enough to withstand the forces imparted on the test vehicle by the deceleration system. The test vehicle and the hardware contained within must allow for repeated testing and the video should be recorded in such a way that it can be analyzed in Matlab. These basic principles and a desire to design a flexible, professional automation system dictated the original design objectives. To this end, decisions were made in the initial design phase which set the course for development and implementation.

The controlling computer selected was the Efika MX microcomputer made by Genesi USA, Inc. It was chosen because of its availability, cost, and functionality. Dr. Kevin Nickels of Trinity University^[5] recommended that the group consider the Efika MX because its robust,

compact design and solid state drive (SSD), would likely withstand the possible deceleration forces. Additional specifications for the Efika MX are available in Appendix A. The specifications pertinent to our application are the amount of RAM (256 MB are required to operate the cameras), the size of the SSD for video storage, and the 2 USB2.0 ports, and wireless capabilities. The 2 USB2.0 ports provide enough bandwidth to trigger the cameras, quick release, and shell deployment and collect video from 2 cameras. Trinity's contact at Genesi USA, Inc., Matt Sealey,^[6] provided technical information and assurance about the Efika MX chances for success in our application during the design phase. The Efika MX was being donated by Genesi USA, Inc, a cost savings of \$250.

With the microcomputer specified, the group decided on a CMOS camera from Mightex Systems because its size, triggering capabilities, USB2.0 connection, low power consumption, resolution, and price. Figure 11 shows a board level version and an enclosed version of the camera selected. The exact camera model is BCE-BG04-U. The camera specifications are available in Appendix A.



Figure 11: Board Level (left) and Enclosed (right) Camera Versions^[7]

Dr. Miles Li^[8] from Mightex Systems recommended this camera based on the requirements of our design. This camera does not require external power, but rather is powered through the USB. It provides more than the minimum 30 fps specified by our project sponsor while achieving a suitable resolution. The cameras are compatible with Linux, the operating system on the Efika MX. Mightex agreed to supply the driver source code for the cameras.

Lenses are not included with the cameras. Based on the minimum object distance (MOD) and field of view of the cameras, a lens was selected based on recommendations by Dr. Li. The MOD and field of view of the cameras are determined by the shell size and test apparatus dimensions. Specifications for the lens chosen are available in Appendix A.

A general purpose I/O device with USB2.0 input was chosen to interface the EfikaMX and the linear actuator used to deploy a mounted, rolled shell. The GPIO device can be programmed by the EfikaMX to output a precisely timed signal to switch a relay that controls the power to the actuator.

2.5.2 Issues Preventing Full Implementation

The expected delivery of the EfikaMX was mid December 2009. However, because of complications at Genesi, the delivery date was pushed back indefinitely. Initially this did not appear to be a problem because, as Dr. Nickels pointed out, the department had an older model Efika microcomputer, the Efika 5200B, that could be used for program development. The specifications sheet can be seen in Appendix E.2. Dr. Nickels said that the programming could be done on the 5200B and copied over to the MX when it became available. At the time, the only pertinent difference between the MX and the 5200B that the group was aware of was the

SSD. As it turned out, the 5200B had much less RAM than the MX. This specification was overlooked and set back programming several weeks.

When the RAM discrepancy was discovered, the group requested a desktop PC from the university. This request took a few weeks to process, further delaying programming. When the computer came in, openSUSE 11.0 was installed, which had been running on the 5200B. OpenSUSE 11.0 runs on kernel 2.6.25 which Mightex stated was being used by satisfied Mightex customers using the cameras purchased. However, the group was unable to run the applications provided by Mightex. The driver and modules loaded successfully but the applications would crash when run. The limited Linux and programming experience of the group made trouble shooting many of the issues that arose in this process very difficult. This limitation was recognized and had expected more helpful and productive support from Mightex and Matt Sealey to make up for this lack of experience. However, this support was unenthusiastic and minimal on the part of Mightex and heavily impeded by external factors on the part of Matt Sealey. The EfikaMX was delivered March 31st with Ubuntu 9.1 (kernel 2.6.32) installed. From communication with Matt leading up to the day he delivered the MX, the group was under the impression he had gotten the driver installed and just needed the cameras to run the provided Mightex applications. This was not the case and another week was spent trying in vain to get the Mightex applications to run on the EfikaMX at which point the group switched back to the desktop because it allowed the freedom to use practically any Linux distribution. Mightex, when directly asked, said the source code and applications they provided were developed for Fedora 5 (kernel 2.6.15) and the patch for kernels 2.6.25 and 2.6.26 was developed by customers for use on those newer kernels. It was decided to install Fedora 9 (kernel 2.6.25) to see if the different Linux distributions, not just the kernels, could be a factor. As it turned out,

this was just the case and with one week left, for the first time pictures were finally taken with the cameras.

Because of the ARM computer architecture on the EfikaMX, it does not currently support all Linux distributions. With the semester ending, the group has had to settle on demonstrating the functionality of the cameras and the programming using a desktop PC running Fedora 9 and leave the full implementation required for a drop test (a microcomputer with a SSD like the EfikaMX) to the Phase II design group. Recommendations for implementation will be discussed in the Conclusions and Recommendations sections. The final automation system design for Phase I is described in the following section.

2.5.3 Phase I Final Design

The final design accomplishes the design objectives as they directly pertain to Phase I; the automation system has a program that triggers a camera which records images that can be analyzed in Matlab and precisely triggers the shell deployment actuator. However, the original objective was for the automation system to ready for actual drop tests to be conducted in Phase II. Due to the many issues described in the previous section and discussed in section 5.4, a drop-ready system was not achieved. The bench top system, the Phase I Final Design, is described in sections 2.5.3.1 and 2.5.3.2 below.

2.5.3.1 Cameras and Mightex App Adjusted Code

The desktop PC used is a Dell GX620 with an Intel Pentium D 2.8 GHz processor and 2 GB of RAM. Presumably any PC with similar specifications would work. The operating system is Fedora 9 (kernel 2.6.25). As mentioned above, this Linux distribution was chosen after much trial and error and it is not clear if it is the only Linux distribution that would work (See

Conclusions and Recommendations section). The original Mightex CMOS camera previously described is used. Source code for the camera driver and an application to capture JPEG images was provided by Mightex. The source code was adjusted by the group and the final code records still pictures at a rate around 60 fps for an adjustable amount of time, triggered by an input to the GPIO. These JPEG images can then later be converted to an AVI file for analysis in Matlab. *were?*

2.5.3.2 Deployment hardware, circuitry, and code

The GPIO used is the Diolan U2C-12 USB-I2C/SPI/GPIO adapter. The general specifications and description are included in Appendix E.7. Diolan provided a header file and a User Manual and Dr. Nickels provided a starter code. Several prototype codes were written to play with the timing sequences and verify output levels. The GPIO pins output 3.3 volts for logic high.

In order to use this output to trigger the linear actuator, a driver circuit was designed that uses the 3.3 volt GPIO output to control a mechanical relay that closes a circuit that powers the actuator with a rechargeable 12 volt lead acid battery rated at 5 Amp-hours. The actuator is rated to draw 3 amps at 12 volts and was taken from the shell deployment system previously designed by Mevicon for their experimental apparatus used on the Vomet Comet.

Also connected to the battery are 3 LED strips previously mentioned in the description of the apparatus in 2.4.1. These strips are connected in parallel to the actuator and draw 120 mA each. The mechanical relay requires a 5 volt control input. To achieve this level using the GPIO output, a Darlington transistor array is included in the design. Both the relay and Darlington array specification sheets are in Appendix E.5 and Appendix E.6 respectively. The driver circuit diagram can be seen in Figure 12 below.

of switch

A detachable wire in parallel with a pull down resistor is used as the input to the GPIO which will trigger the shell deployment. The code for the timing sequence waits for a logic low input to trigger the delayed GPIO output described above.

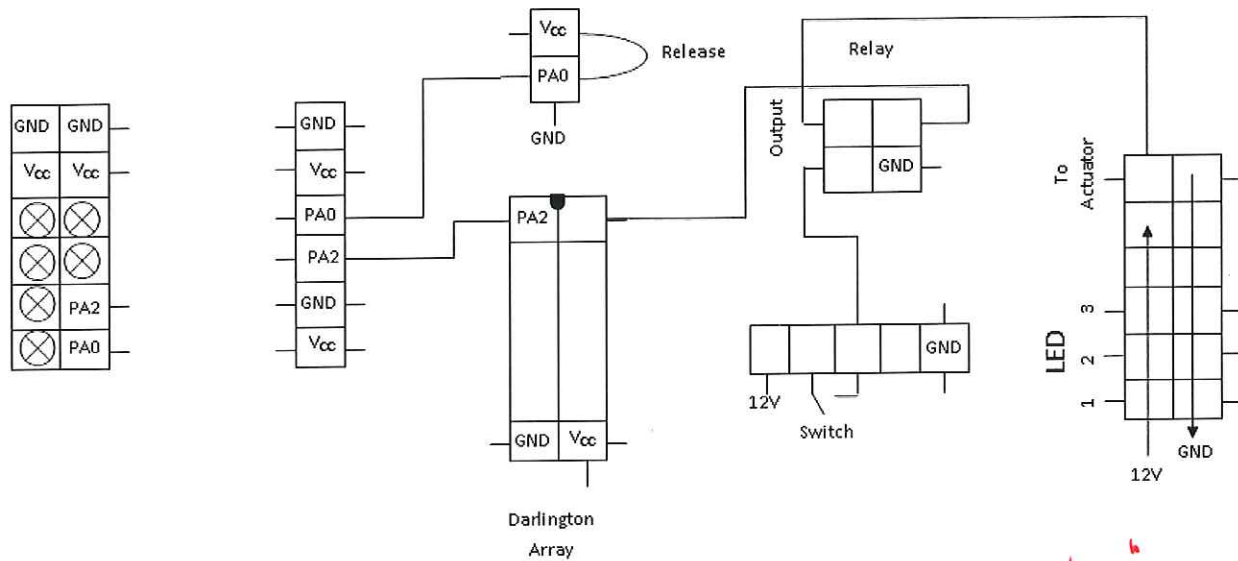


Figure 12: Driver Circuit

add schematic

3 Methods

The Methods section describes the deceleration system tests and the analysis performed on the drop apparatus.

3.1 Deceleration System

A deceleration system was constructed with a total of 12 ft available for dropping. The dummy load was given 3 ft, 6 ft, or 9 ft of freefall and was decelerated in the remaining distance by a varying counterweight ranging from 2.22 lbs/ft to 15.54 lbs/ft. The dummy loads dropped weighed 5 lbs, 10 lbs, 15 lbs and 20 lbs. Each experiment was repeated at least 3 times for consistency. The test matrix for the prototype deceleration tests is shown in Appendix G. During each test, one person handled the camera for recording the drop while the other person set up the load for drop and dropped it using the eye-bolt release mechanism.

The captured video was imported to MATLAB for analysis. A conversion factor converts pixel distances in the video to actual distances. Refer to Appendix A for a better explanation of data collection. This data collected was exported into Excel sheets for plotting and analyzing. Freefall and deceleration stages of drop was distinguished by checking the rate of change of distance and by using frame by frame visual analysis of recorded video. The results from data obtained were then compared with the model.

3.2 Apparatus System – ProMechanica

As stated previously, the most important function of the apparatus is to withstand repeated drops from the specified drop height, while keeping all electrical components held within completely intact and unaffected. This means that the apparatus must be strong enough to withstand the forces during deceleration. As the final drop height, and means of decelerating the

apparatus have not been yet determined, the exact forces during deceleration are unknown. These decisions will be made by a later design group continuing the project. However, models have been made using Newton's law to estimate the forces that the apparatus will encounter for required free fall drop lengths of 2 seconds and using a chain as a means of counterweight deceleration. With these models, and the drawing completed in ProEngineer, ProMechanica was used as an attempt at a finite element analysis of the forces on the individual pieces of the apparatus. The group had much difficulty getting ProMechanica to complete a dynamic analysis of the complex model. The program continued to crash after running a single analysis for 8 to 12 hours. Because of this, a simpler model of the apparatus was drawn using solid strut pieces and corner cubes. This model was to scale with the more complex model, but did not include the intricacies of the Bosch strut design. An image of this simpler model with applied ProMechanica materials, loads and constraints can be seen in Figure 13.

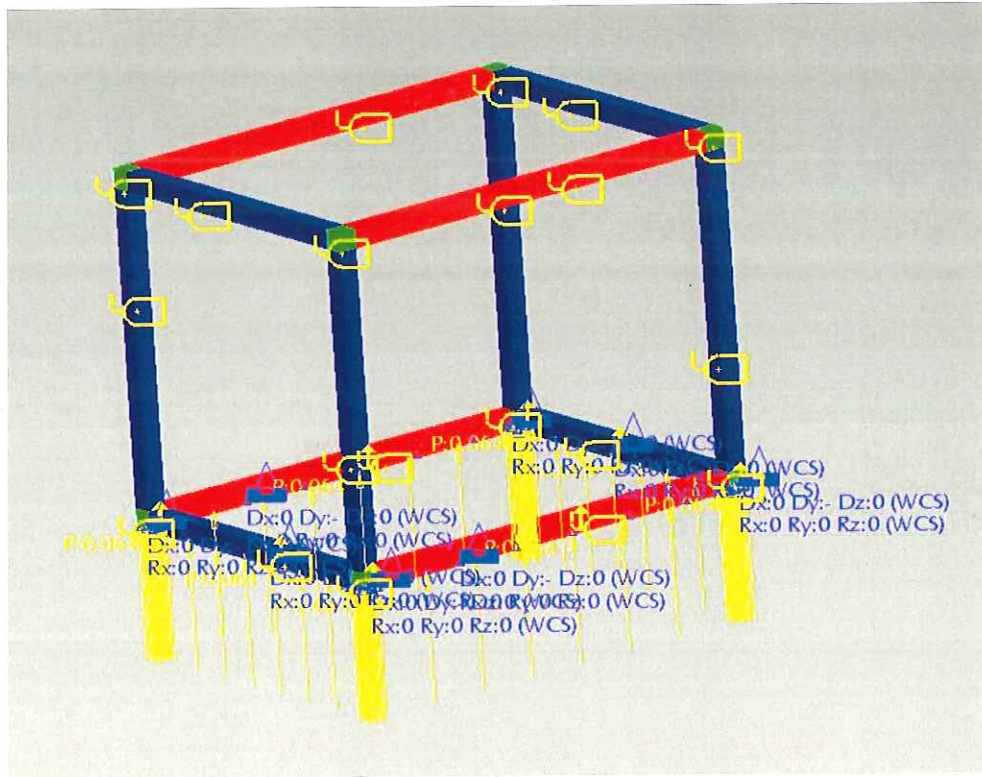


Figure 13: Simplified Apparatus Pro E Drawing

4 Results

After much recording and data conversion as well as ProMechanica simulation, the group has come to the following results.

4.1 Deceleration System

After the drop test videos were converted to quantitative data and plotted, each set of runs were compared to the ideal model. A velocity plot of a dummy weight of 15 lbs in freefall can be seen below in Figure 14.

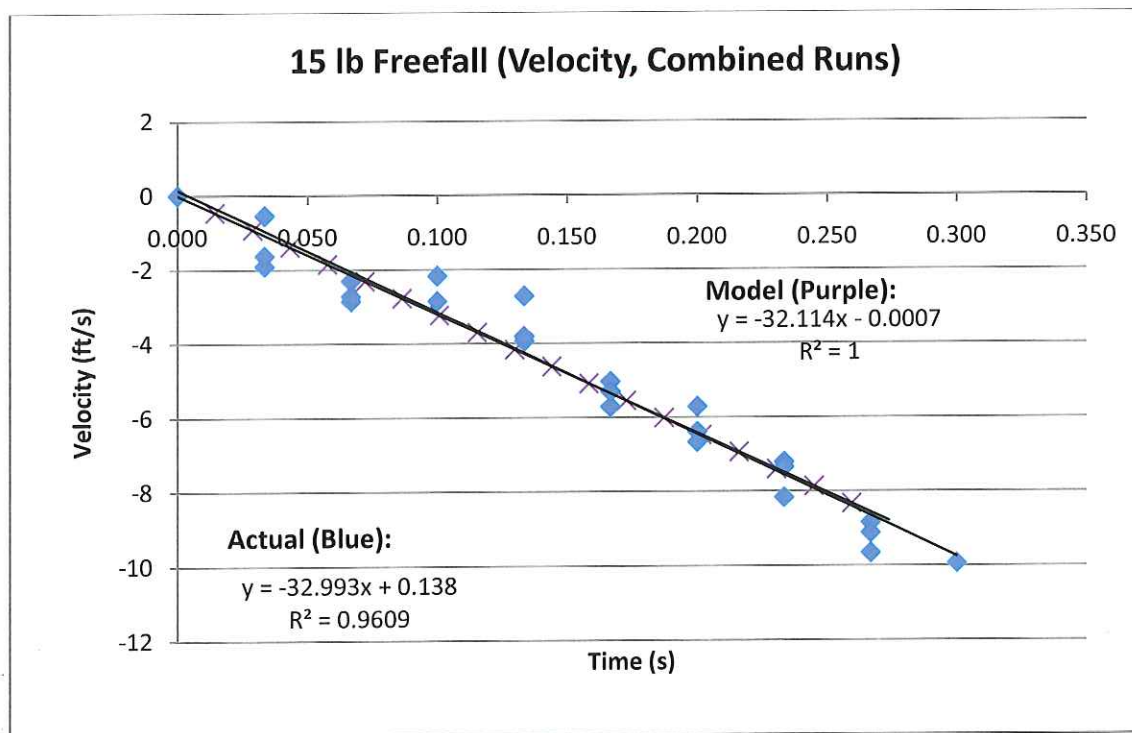


Figure 14: Plot of 15 lb Object in Freefall, Actual Results vs. Model

In the majority of the test runs, the dummy weight turned over on itself during freefall, causing false interpretation when detecting the center of the mass where the majority points were recorded. Although sometimes this causes the velocity plots to be extremely erratic and inaccurate, the flipping of the dummy weight can be seen in Figure 14 between 0 and 1.5 seconds. It is seen that the resulting calculated acceleration is 32.993 ft/s^2 , which is optimal considering the rough video to quantitative data conversion. However, in other cases, the acceleration during freefall is observed to be significantly larger than the ideal case, such as one involving 5 lbs of dummy weight as can be seen below in Figure 15.

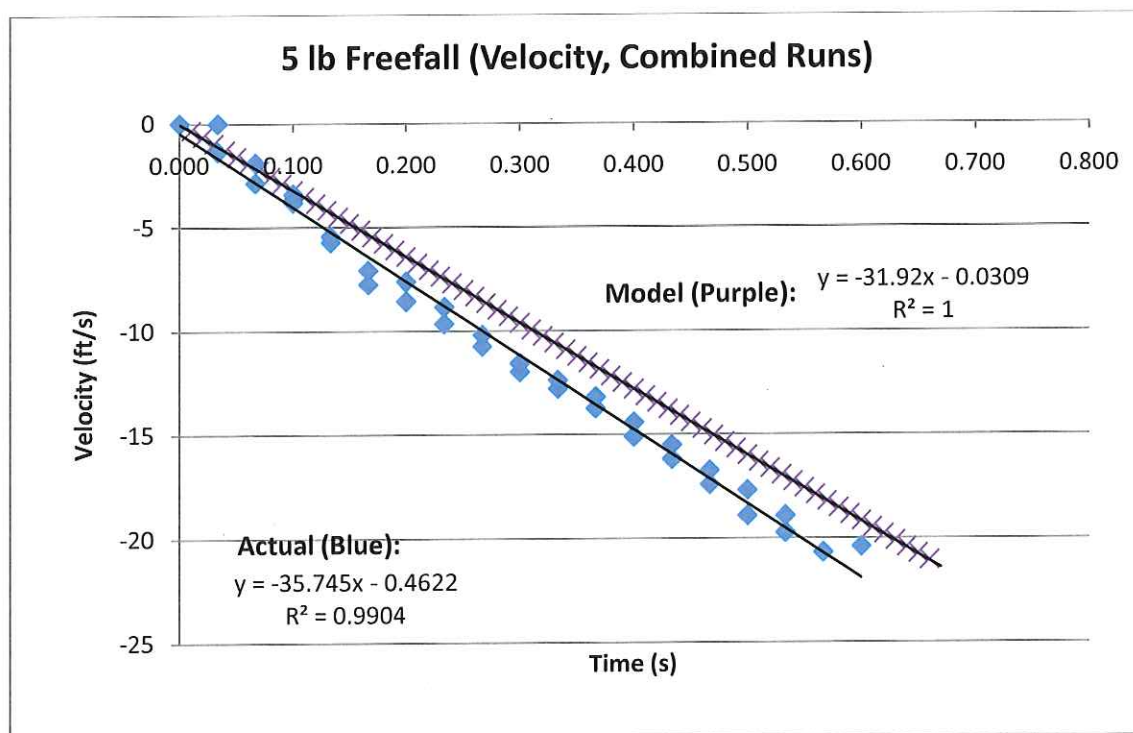


Figure 15: Plot of 5 lb Object in Freefall, Actual Results vs. Model

While the average acceleration of the ideal model is 31.92 ft/s^2 , (Less than the common 32.3 ft/s^2 due to six feet of drag forces) the acceleration of the data is averaged at a high 35.745

ft/s². The deceleration data for this test indicates that the dummy weight finally came to rest after deceleration at approximately 1.395 feet above the ground. However, it was measured and noted during testing and recording that the object came to rest at 0.541 feet, a significant difference of 10.24 inches.

It was also noticed that the data indicates that the dummy load was dropped at approximately 10.224 feet, yet it was measured during testing and recording that the object was dropped at 10.041 feet, a difference of 2.196 inches. The discrepancies in high acceleration and both initial and final position points to possible pixel conversion or camera calibration errors for some tests. Despite these issues, the general shape of the prototype plots and model plots for these tests may still be compared.

After observing several runs during recording, it became evident that, although the freefall appeared to represent the computational model, the deceleration did not execute as expected. The dummy load came to rest significantly more quickly, and thus in a smaller distance than predicted by the model, as seen in Figure 16.

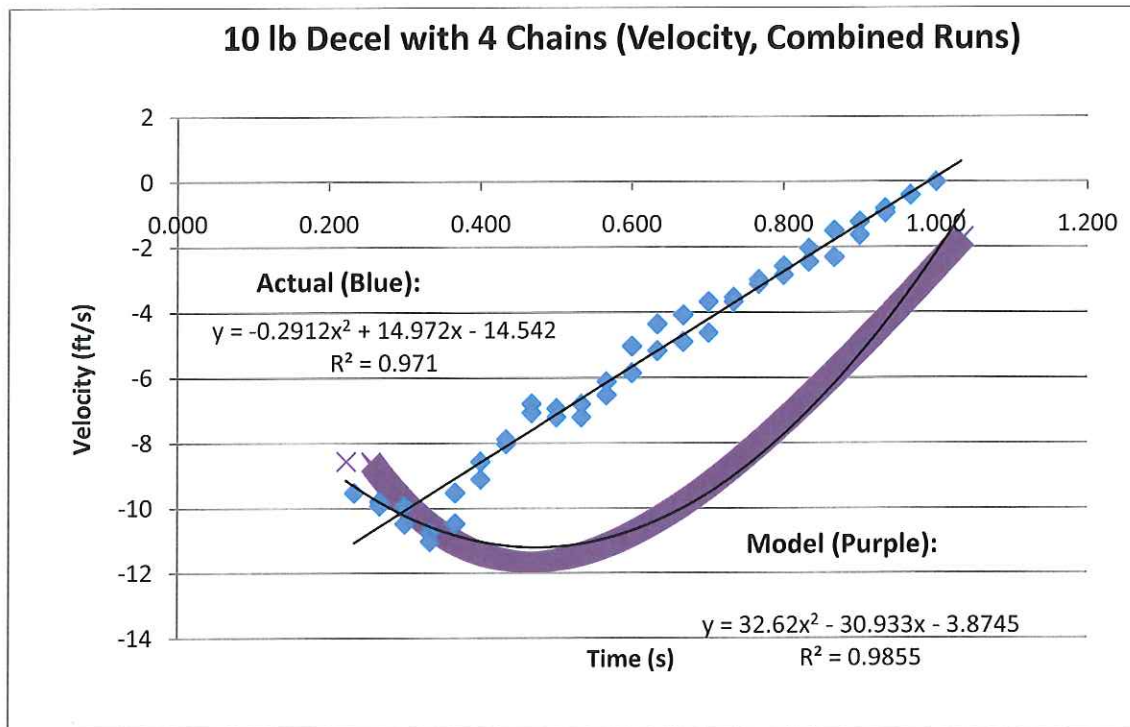


Figure 16: Plot of 10 lb Object in Deceleration after 3 Feet of Freefall, Actual Results vs. Model

As the chain begins being pulled off the ground, it counters the weight of the dummy load. With enough chain, the dummy weight reaches its maximum speed and begins to slow. In Figure 16, the dummy load attains this maximum speed after a tenth of a second of deceleration, while the model reaches its maximum speed a tenth of a second later. Although this seems negligible, differences like these cause the model to travel 2.72 feet farther than the prototype before coming to rest, a significant amount when considering the total height is only approximately 11 feet.

Another commonly seen trend can be found when viewing the deceleration plots after 9 feet of freefall, leaving only 3 feet for deceleration. An example of this plot can be seen in Figure 17.

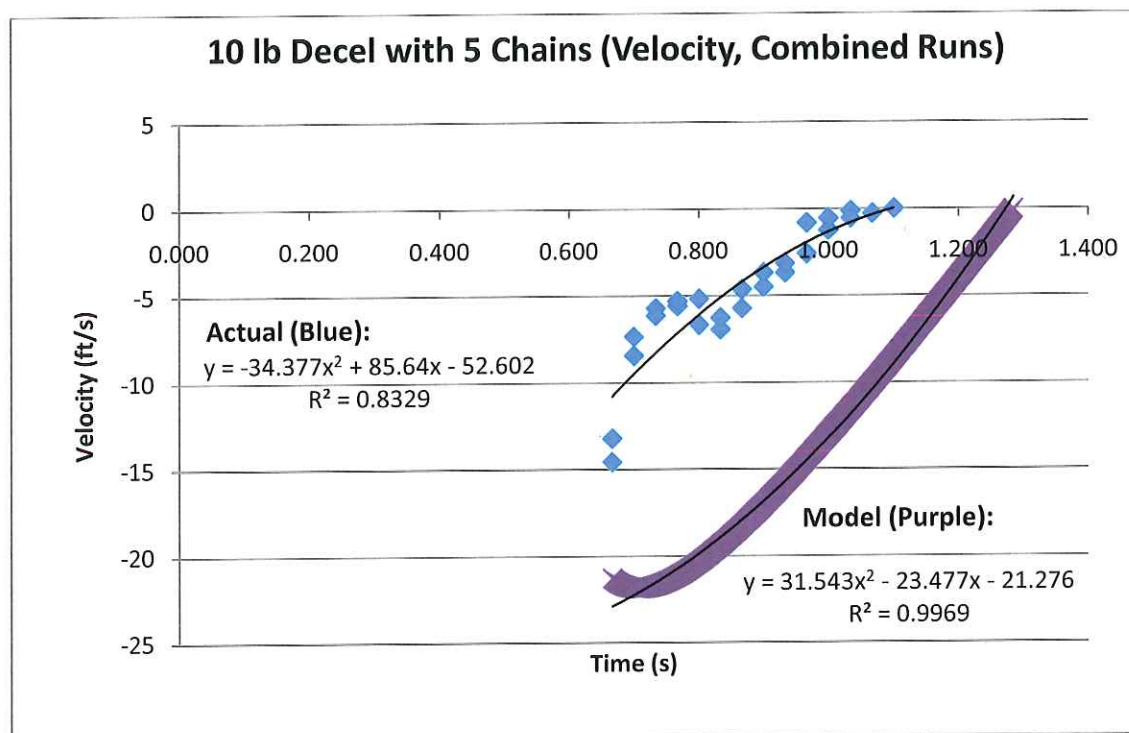


Figure 17: Plot of 10 lb Object in Deceleration after 9 Feet of Freefall, Actual Results vs. Model

This plot shows an immediate jump in velocity from almost 15 ft/s to nearly 5 ft/s in a tenth of a second in the prototype data. This trend is observed in every deceleration plot where the dummy load is dropped in freefall for 9 feet, whereas in 6 feet of freefall and 3 feet of freefall, the plots have similar trends to the model. These velocity models have been derived by taking the derivation of the position points with respect to time. The position points can be seen in Figure 18.

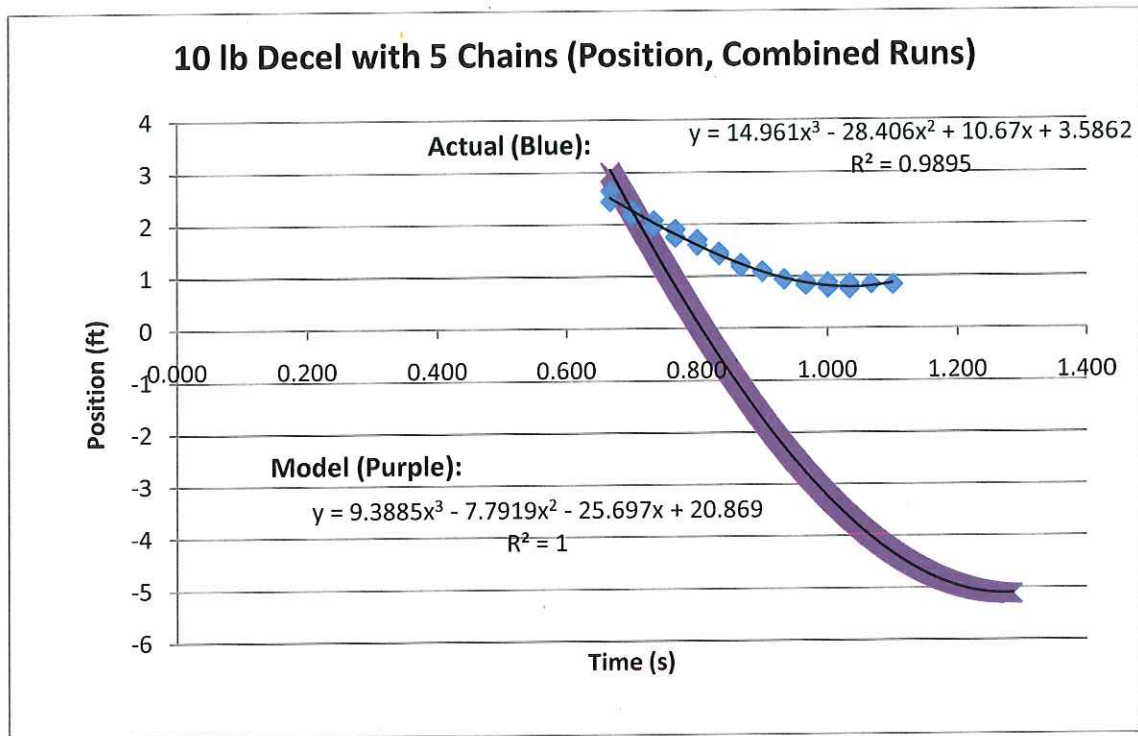


Figure 18: Plot of 10 lb Object in Deceleration after 9 Feet of Freefall, Actual Results vs. Model

Figure 18 shows a much smoother collection of data. Taking the derivative of the trendline equation results in a far cleaner and upwards concaving line for acceleration, which is considered to be the accurate acceleration trend for this run. Although the video yielded smooth position points, the successive point derivation showed that even with an error of one or two inches, it is not an accurate method to model velocity.

4.2 Apparatus System – Simple Model

Dynamic analysis on the simplified model eventually yielded results. These results however, are not as expected and altogether do not appear accurate. The estimated yield stress

for a 1000N force over a 40mm x 40mm surface is 0.625 MPa. It is stress turnout from the ProMechanica analysis is expected to be 20% of the yield stress, approximately 0.125 MPa. The resulting stresses, as low as 1×10^{-9} MPa are grossly inaccurate. Research concerning beams and other applications in ProMechanica was performed, but reasonable results were not found.

5 Conclusions and Recommendations

The following sections detail the successes and failures of each subsystem with respect to the design objectives. Generally speaking, a functional bench-top apparatus and automation system have been achieved but the group did not achieve its goal of producing a drop-ready system. Prototype tests yielded useful information about the behavior of the differential counter mass deceleration method, though further testing and modeling could provide additional design considerations

5.1 *Deceleration Model and Prototype*

As previously mentioned, the camera only views real distance perfectly in line with its vision. When tracking the dummy load higher or lower than its own lens height of 53 inches, the ratio of pixel height to actual height decreases with each pixel. When the video was converted to quantitative data, the conversion factor of pixel to inch had a standard deviation of error of 0.2464, apparently miniscule yet evidently too large for the task at hand. With this realization, it is difficult to determine the accuracy of the results. Thus, it is questionable if the resulting calculated position, velocity, and acceleration values are correct. With a smaller standard deviation of error, results will be far more accurate.

In addition to the error in the video conversion factor, the friction in the pulleys play a significant role in the unexpected prototype results. Friction in the pulleys was not taken into account when creating the model. With an extremely complex differential equation and unknown friction factor, attempts to model friction were abandoned. Although the pulleys chosen have ball bearings with low friction, the friction still plays a substantial role. Fortunately,

the purpose of our prototype is to stop a falling mass via counterweight, and the friction only helps in this role. The results of the model give a worst case scenario situation. In other words, in a realistic application, the falling mass will stop before indicated in the model. The downside is this allows for less accurate prediction of allowed freefall distance and imprecise calculation of the total tension in the cable and force on the pulleys and load.

The extreme jump seen in all of the deceleration plots after 9 feet of freefall has been ignored. Initially it was thought that this was due to the assumptions concerning the chain. In order for the model to be accurate, the chain links are assumed infinitesimally small with an essentially consistent mass; however the actual chain links do not have constant mass, which might make the dm/dt term larger than predicted in the model. However, it is unlikely that this would make such a large impact on the data. More realistically, because the velocity has reached over 20 ft/s after traveling 9 feet in freefall, it is difficult to accurately capture the exact position of the weight with a camera at 30 frames per second. It is recommended for future analysis that the successive differentiation of points be ignored, and to rely solely on the derivative of the position trendline to determine respective velocities. It is also recommended that for tests with high velocities, the data be recaptured by a camera with a faster frame rate. This will allow a larger amount of data points with less time in between each for more accurate results.

5.2 Recommendations for Measuring Techniques

The number of data points that can be recorded are limited by the frame rate. For a greater frame rate, either a faster camera has to be used, or repeated measurements have to be performed and the data from these measurements have to be aligned and combined. The program that was written for analyzing the video data involved adjusting several thresholds values that helped to either recognize the object or helped to eliminate noise. Therefore, the quality of the

data cannot be improved without finding better equipment or putting in extra work. One advantage of using the video technique is that it can be set up with least interference to the experiment. Another advantage is that this technique can be used to take “swinging” into account by measuring the horizontal displacement of the object in addition to the vertical displacement.

The maximum distance that was required to be measured was only about 12 ft. If a greater distance measurement is required, it is recommended that more cameras are used. The cameras can be set up at different elevations and be set up to measure distances to a common frame of reference so that the data can be combined easily. While the experiment is performed, it is recommended that the number of non-stationary objects be reduced and that the intensities of extraneous objects be distinct from the object of concern. This will enable easier implementation of filters. To prevent blurring of images while the object is falling, it is recommended that a high shutter speed with lots of light be used. The object that was dropped in our experiment was a flat barbell plate. Although preventive measures were taken, the object would rotate while it was dropping, resulting in a smaller, thinner interpretation since it was viewed from the side. For future prototype tests, it is recommended that a spherical object be dropped so that the effects of rotating is eliminated. Although, a constant conversion factor did not seem to effect the accuracy of the data significantly our set up, future groups should study the effects of this for their setups.

Measuring the distance of drop using the video technique is a tedious process and involves adjusting several parameters. If future groups do decide to continue using this method, they should be aware of the precautions and complexities involved. There are several off the shelf techniques in the market that can be used for measuring drop distance. They include high end ultrasonic and laser devices to simple ticker tapes. The group decided to use the video technique because it reduced the interference of the measuring device on the dropping load. If in

the future, the mass of the drop load is increased, the effects of measuring devices such as ticker tapes can be assumed to be negligible.

5.3 Apparatus System

Although the group is extremely confident with the structural integrity of the apparatus, testing results are inconclusive at this time. Having simplified the model to a level where the program was able to yield results, they were either inaccurate or misinterpreted. The group made the decision to stay with Bosch prefabricated aluminum strut, order the pieces, and assemble the apparatus based on the assumption that the analysis in ProMechanica will eventually yield accurate results. The choice to stay with Bosch was made because if these results end up showing a lack of structural integrity due to the forces during deceleration, Bosch has components for reinforcing the connections of the frame.

The corner cubes used to connect the frames of the box are listed with a load carrying capacity of 70 Nm.^[9] The exact forces on the frame during deceleration have not been calculated yet, but if they were to surpass this moment limit, there are other options for reinforcing the connections of the frame. One such option is a right angle gusset which is listed as having a load carrying capacity of 3000 N.^[9] An image of which can be seen below in Figure 19.

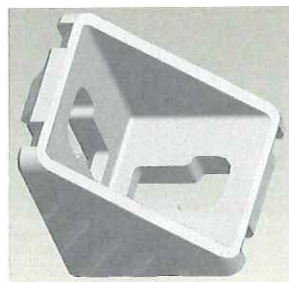


Figure 19: Right Angle Gusset^[3]

As stated previously in the paper, budgetary issues and time constraints have limited construction of the apparatus to not include mounting of the Efika microcomputer, related electronic components and power supplies, as well as the housing for enclosing the structure. Along with reimbursement issues concerning the Mightex cameras that will be discussed later, other budgetary problems arose when returning the 50 foot chain used in the deceleration testing to Grainger. After testing was completed, it was decided to return the 50 foot chain to Grainger, and using the refunded amount of \$237.60, purchase the aluminum material for enclosing the apparatus as well as the electronics box for mounting the electrical components within. The purchase of the chain was made through a Trinity account pre-established at Grainger, and when the chain was returned, the refund was credited to this account for future purchases, and was not distributed back as a cash sum. Because of this unforeseen issue, amounts were not available for additional purchases. A recommendation for future large purchases made at Grainger, or any supplier is to make such purchases using a credit card and not an account, allowing for reimbursement for returns if necessary.

Rent of
Chain?
Ethical
Issues?

Research has been done to ensure that these tasks can easily be completed in the next year's senior design group. Grade 16 aluminum sheets made by West Brooks Metals in San Antonio were chosen to enclose the apparatus. Contact information, sizing, and a cost breakdown for different grades of aluminum sheeting can be found in Appendix F. These sheets can be precut at West Brooks Metals and can be connected to the apparatus using the already purchased T-Nuts at the corners and in the middle of the longer strut lengths to ensure a tight and fully enclosed fit. The sheets will need holes drilled at the appropriate locations to allow screws to connect to the T-Nuts that easily slip within the grooves of the strut material. The T-Nuts

have ¼"-20 threading and require the appropriate screws. The enclosure material does not have to be excessively robust as the forces on this apparatus will predominantly be absorbed by the prefabricated frame. The enclosure does however need to be as tightly fit to the apparatus as possible to ensure uniform lighting of the shells.

The design for housing the Efika microcomputer, related electronic components and power supplies included securing them in a prefabricated electrical box, padded to ensure the safety of the components during deceleration. The box would then be bolted to the strut to ensure a secure fit during deceleration. Additional strut pieces have been purchased as well inside-to-inside gussets, for connection to the frame, and T-Nuts, to allow more secure support of the base of the box. Enough room has been allowed within the apparatus for multiple prefabricated box sizes to be used. These can be purchased directly from Intertex Systems, or ordered from multiple catalogs including Allied electronics.

5.4 Automation System

First and foremost, the automation system is incomplete because it is not ready for a drop test. The issues preventing implementation of the EfikaMX limited the Phase I automation system to a bench top system able to demonstrate the functionality of the cameras, the GPIO, and the driver circuit. Phase II of this project will have the additional task of integrating the EfikaMX with the design or exploring the possibility of a different automation system.

The original design objectives required that the "components of the automation system, particularly the controlling computer and the cameras, must be robust and shock resistant enough to withstand the forces imparted on the test vehicle by the deceleration system." From the above design description it is quite obvious this objective was not achieved. However, aside from the failure to incorporate the EfikaMX, the rest of the design meets that criterion. Additionally, the

system achieves the required frame rate and professional quality desired, is repeatable, and flexible.

Not anticipating the compatibility problems of the EfikaMX and the cameras was an oversight of the group. In the attempt to design a professional quality system, our group unintentionally overreached into areas outside our experience. Unforeseen complications were run into because the group did not know the right questions to ask. The next few paragraphs describe potential directions future work can explore.

The Phase II group will have to look at the Phase I automation system and decide whether they want to pursue the EfikaMX as the microcomputer for the ultimate drop-test ready system. The benefit of using the EfikaMX, of course, is that it is free and on hand. However, integrating the EfikaMX with the current system will require much help from a Linux guru and Mightex which our experience has shown to be very difficult to obtain. Mightex proclaims a commitment to customer service, however, after our purchase was finalized, the quality of customer service dropped off dramatically. The only technical support received were short, unenthusiastic e-mail responses with very general and ambiguous responses to direct inquiries. On top of that, all communication went through a customer service representative instead of direct communication with the engineers or technical team. If Mightex is willing to provide source code compatible with Ubuntu or a Linux distribution compatible with the EfikaMX, integrating the Efika would be a very easy straightforward task. However, if they do not, serious code adjustment will be required which the group does not believe is possible for even an above average student. A software developer like Matt Sealey willing to devote serious time would be required. While Mr. Sealey is very capable and made what appeared to be sincere efforts to help our project, however, he is working and going to school and is not readily available. He would

need to come work with the cameras and the EfikaMX at Trinity for multiple sessions of several hours. This seems like a long shot.

Another option is to find different cameras that will work with the EfikaMX. This is a real possibility, though potentially an expensive one. A Linux compatible webcam could be used with the EfikaMX if one were found that met the resolution and frame rate requirements.

Cameras similar to the Mightex cameras are likely available, though very vigilant research is recommended to be done to ensure compatibility with the ARM core architecture of the EfikaMX and the Ubuntu distribution. A spec sheet of the cameras and a spec sheet of the EfikaMX were provided to Matt Sealey and Mightex, respectively, and both assured the cameras and EfikaMX would be compatible. This turned out to not be true.

Another option is to find cameras that can be controlled and record video without a computer, such as a robust, shock resistant handcam. This would allow the EfikaMX to be used to operate only the GPIO. Though, if the cameras do not require a computer, the EfikaMX is overkill for controlling the actuator. There are several cheaper, simpler alternatives to the EfikaMX for just controlling the actuator like a PLC or FPGA.

If a microcomputer can be found that has a SSD and can run Fedora 9 or earlier (something with x86 PowerPC architecture), this could also be a solution. The EfikaMX would have cost around \$250 and one could expect similar microcomputers to cost about that much.

1/15/10
This possible solution is the recommendation of this group. Though, as mentioned above, the assurances of suppliers that their systems will be compatible have to be taken with a grain of salt.

It is important to know what questions to ask and not to attempt an approach or design plan that relies heavily on the support of experts, particularly if you are not paying them for their

(J. J. J. J. J.)

time. Unless there is a contractual commitment from someone, there is no guarantee they will follow through on their promises.

6 Bibliography

1. **Dubose, Travis.** *Mevicon*. 2009.
2. **Leva, Scott A.** November 2, 2009.
3. **Bosch Rexroth Corporation.** *Bosch Rexroth Corp.* [Online] 2001.
<http://www.boschrexroth-us.com>.
4. **Edmund Optics Inc.** English and Metric Bench Plates. *Optics, Imaging, and Photonics Technology*. [Online] Edmund Optics Inc., 2009.
<http://www.edmundoptics.com/onlinecatalog/displayproduct.cfm?productID=1349>.
5. **Nickels, Kevin.** Associate Professor, Trinity University. Fall 2009.
6. **Sealy, Matt.** Product Development Analyst, Genesi USA, Inc., E-mail conversations. Fall 2009.
7. **Mightex Systems.** Wide VGA 752x480 Monochrome 8-bit CMOS Cameras with Global Shutters and 32MB on-Board Memory. *Mightex Systems*. [Online] Mightex Systems, 2007. http://www.mightexsystems.com/family_info.php?cPath=1_51&categories_id=51.
8. **Li, Miles.** Mightex Systems. E-mail conversations. Fall 2009.
9. **Rexroth -- Bosch Group.** Aluminum Structural Framing System. *Everything to Build Anything™*. 2007, Vol. 6.0, Catalog.
10. **Genesi USA, Inc.** EFIKA MX Open Client. *Genesi*. [Online] Genesi USA, Inc., 2009-2010. <http://www.genesi-usa.com/products/efika>.

A Drawings

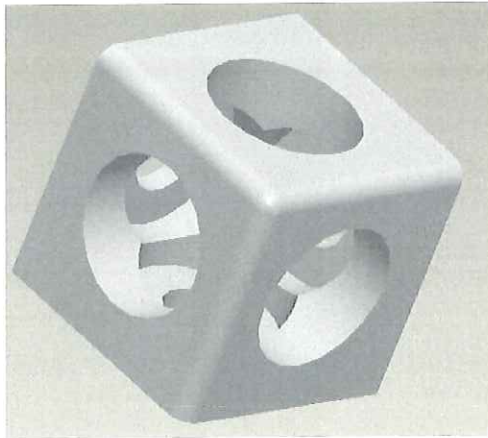


Figure A-1: Corner Cube ^[3]

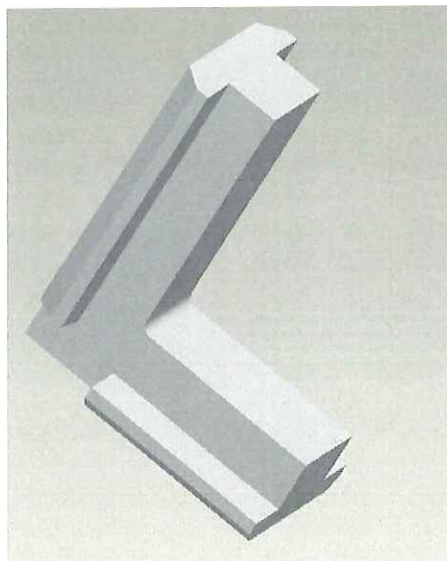


Figure A-2: Inside-to-Inside Gusset ^[3]

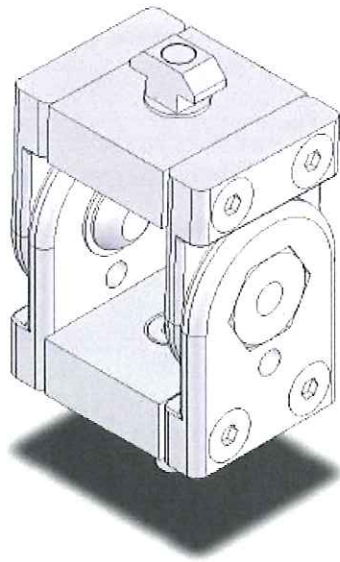


Figure A-3: Multi Angle Fastener^[3]

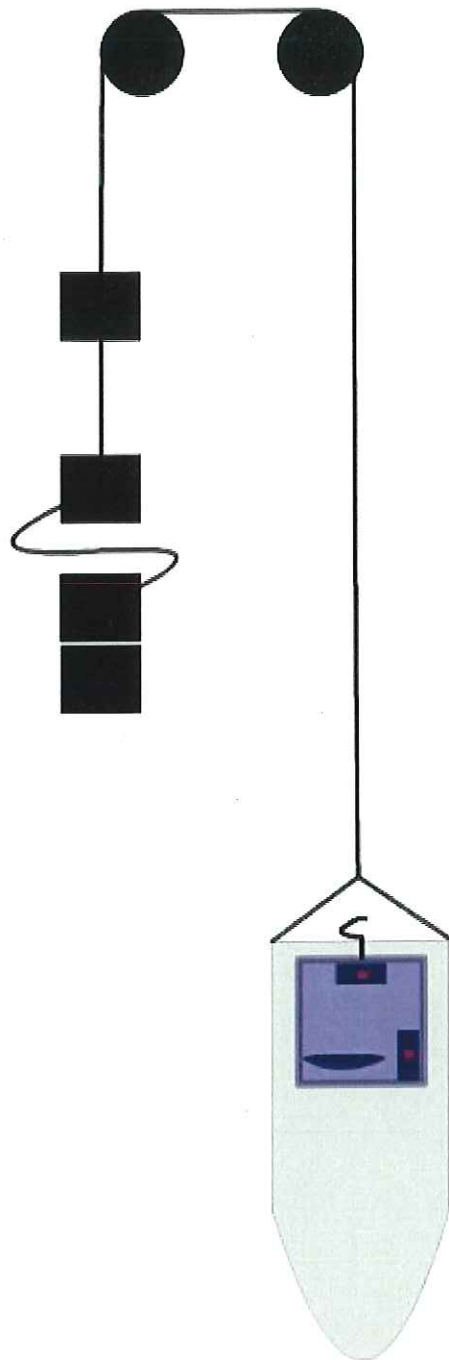


Figure A-4: Schematic of Counter Weight Decelerating System

B Plots

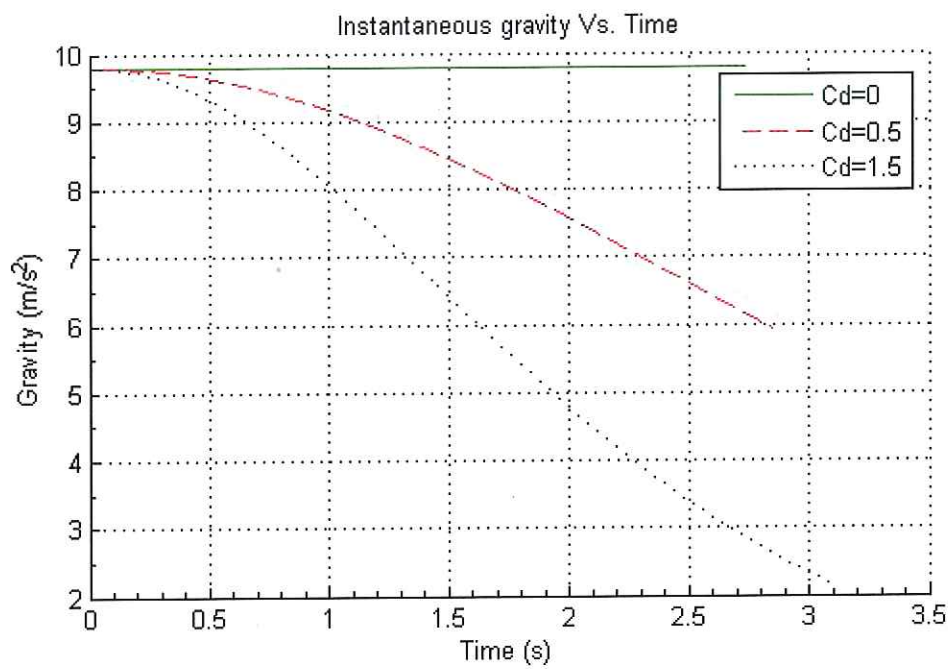


Figure B-1: Acceleration due to gravity felt vs. Time for different drag coefficients

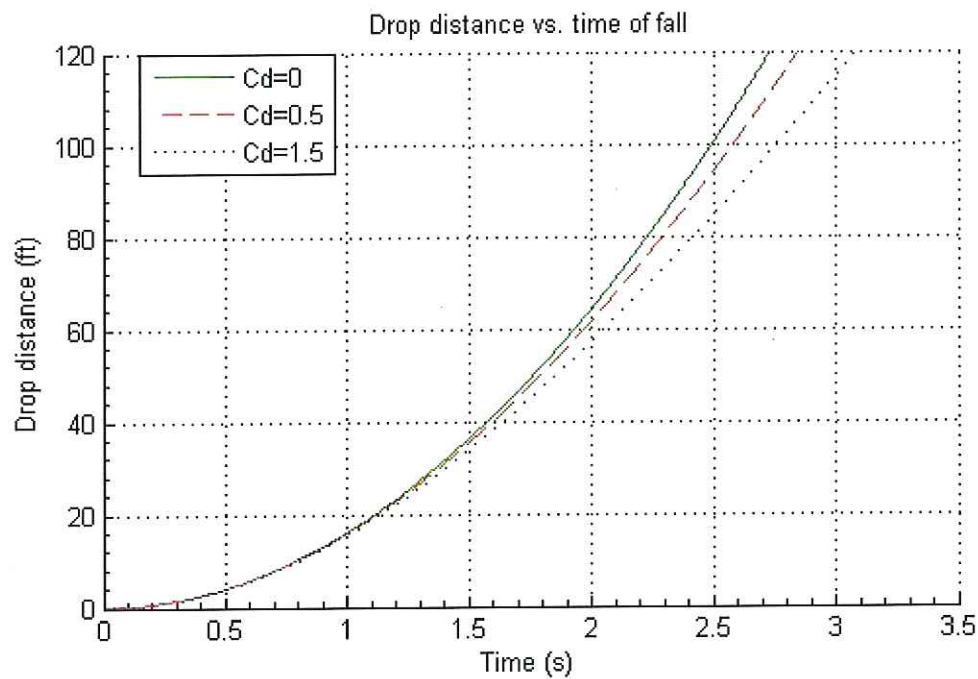


Figure B-2: Drop distance vs. Time for varying drag coefficients

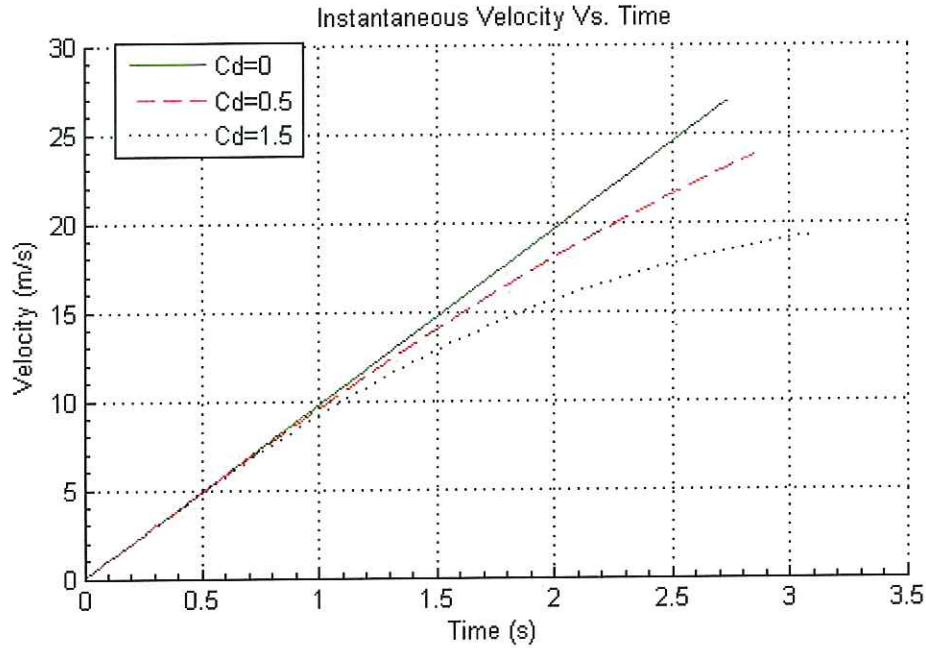


Figure B-3: Velocity of falling object vs. Time for varying drag coefficients (C_d is drag coefficient)

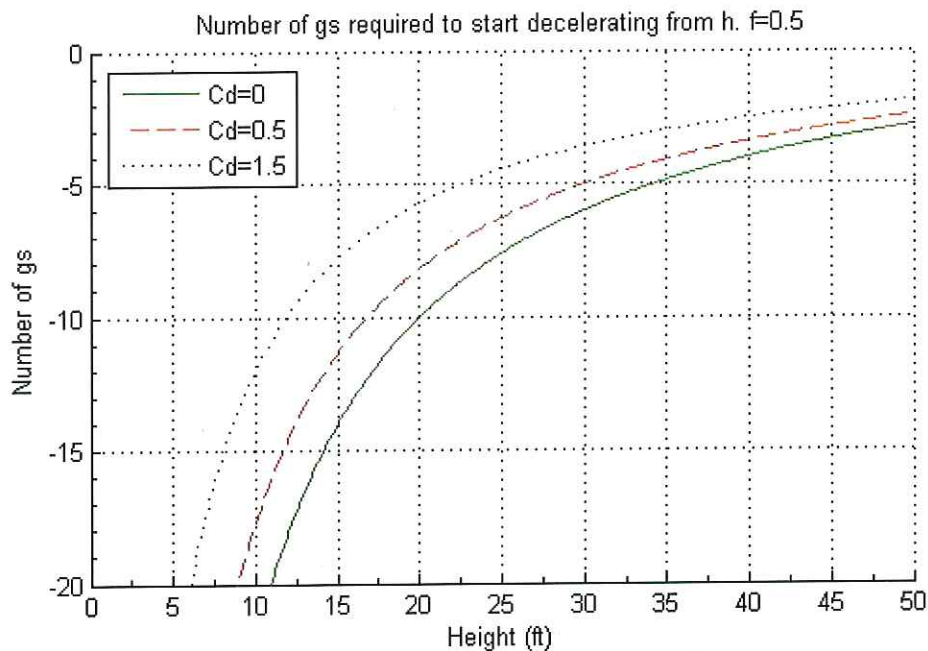
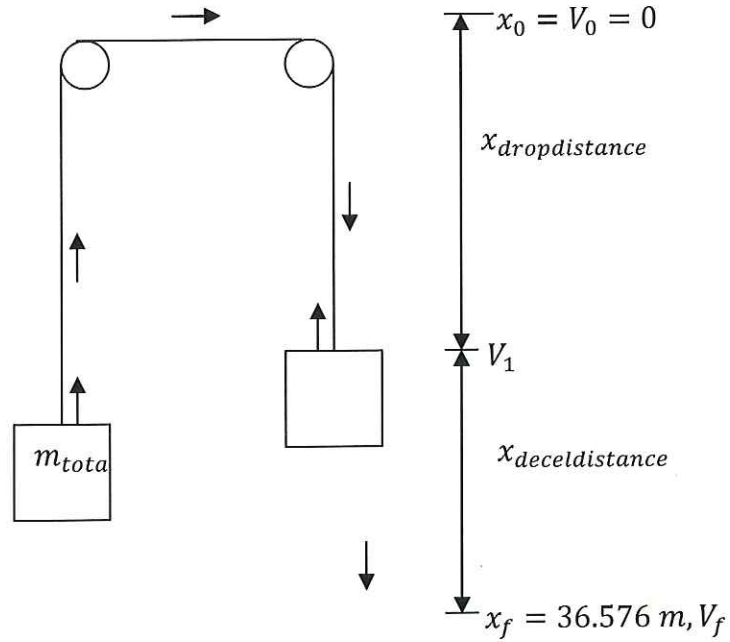


Figure B-4: Number of Gs required to decelerate a 100kg mass that was dropped from 120 feet given that that deceleration starts from at a height of 'h' feet and only 'h*f' feet is available for deceleration

C Calculations

C.1 Freefall Calculations (Without chain)

Reference sketch for calculations:



Drop calculations:

Equation parameters:

$$\mu = \text{sqrt}\left(\frac{g}{\text{lambda}}\right) \quad (\text{C-1})$$

$$\lambda = \text{rho} * A * \frac{C_d}{2 * m} \quad (\text{C-2})$$

Instantaneous velocity during drop:

$$V_{\text{duringdrop}} = \mu * \tanh(\lambda * \mu * t) \quad (\text{C-3})$$

Instantaneous acceleration during drop:

$$a_{\text{duringdrop}} = g - \lambda * V_{\text{duringdrop}}^2 \quad (\text{C-4})$$

Instantaneous position during drop:

$$(\text{C-5})$$

$$x_{duringdrop} = \frac{\ln(\cosh(\lambda * \mu * t))}{\lambda}$$

Drop distance:

$$x_{dropdistance} = x_1 - x_0 \quad (C-6)$$

Time of drop:

$$x_{dropdistance} = \frac{\ln(\cosh(\lambda * \mu * t_{drop}))}{\mu} \quad (C-7)$$

C.2 General Deceleration Calculations

Velocity at top of deceleration:

$$V_1 = \mu * \tanh(\lambda * \mu * t_{drop}) \quad (C-8)$$

Tension (Force balance):

$$Tension - m_i * g = \frac{dm_i * v}{dt} \quad (C-9)$$

$$-m_{total} * a_{decel} = m_{total} * g - Tension \quad (C-10)$$

$$M * a_{decel} = M * g - Tension \quad (C-11)$$

Deceleration necessary to stop apparatus:

$$V_f^2 = V_1^2 + 2 * a_{decel} * (x_f - x_1) \quad (C-12)$$

Instantaneous velocity during decel:

$$V_{duringdecel}^2 = V_1^2 + 2 * a_{decel} * (x_{duringdecel}) \quad (C-13)$$

Time for deceleration to stop apparatus:

$$(x_f - x_1) = V_1 * t_{stop} + 0.5 * a_{decel} * t_{stop}^2 \quad (C-14)$$

Instantaneous position during deceleration:

$$(x_{duringdecel}) = V_1 * (t - t_{drop}) + 0.5 * a_{decel} * (t - t_{drop})^2 \quad (C-15)$$

Distance of deceleration:

$$x_{deceldistance} = x_f - x_1 \quad (C-16)$$

Number of g's:

$$N_g = a_{decel} * \frac{-1}{g} \quad (C-17)$$

C.3 Exact Solution of Deceleration Model

$$a_A \left(\frac{y}{2} + y_A \right) + \frac{1}{2} (v_A)^2 + g(y - y_A) = 0 \quad (C-18)$$

Since, $a_A = v_A \frac{dv_A}{dy}$, the equation can be rewritten as,

$$v_A \frac{dv_A}{dy} \left(\frac{y}{2} + y_A \right) + \frac{1}{2} (v_A)^2 + g(y - y_A) = 0 \quad (C-19)$$

$$\Rightarrow \frac{dv_A}{dy} \left(\frac{y}{2} + y_A \right) + \frac{1}{2} (v_A) + g \frac{(y - y_A)}{v_A} = 0 \quad (C-20)$$

$$\Rightarrow \frac{dv_A}{dy} + \frac{v_A}{2 \left(\frac{y}{2} + y_A \right)} + g \frac{(y - y_A)}{v_A \left(\frac{y}{2} + y_A \right)} = 0 \quad (C-21)$$

Using Integrating factor $= 2 \left(\frac{y}{2} + y_A \right)$, the first two terms merge and the equation looks as follows:

$$\frac{dv_A \left(\frac{y}{2} + y_A \right)}{dy} + g \frac{(y - y_A)}{v_A} = 0 \quad (C-22)$$

$$\text{Let } v_A \left(\frac{y}{2} + y_A \right) = P$$

$$\frac{dP}{dy} + g \frac{(y - y_A) \left(\frac{y}{2} + y_A \right)}{P} = 0 \quad (\text{C-23})$$

$$\Rightarrow \int P dP = -g \int (y - y_A) \left(\frac{y}{2} + y_A \right) dy \quad (\text{C-24})$$

$$\Rightarrow \frac{P^2}{2} = -g \left[y \left(\frac{y^2}{6} + \frac{y_A y}{4} - y_A^2 \right) + C \right] \quad (\text{C-25})$$

$$\Rightarrow v_A^2 = \frac{-2g \left[y \left(\frac{y^2}{6} + \frac{y_A y}{4} - y_A^2 \right) + C \right]}{\left(\frac{y}{2} + y_A \right)^2} \quad (\text{C-26})$$

When $y = 0$, $v_A = v_F$, or the final velocity from freefall. Therefore $C = -\frac{v_F^2 y_A^2}{2g}$

Now, $v_A = \frac{dy}{dt}$, and

$$\frac{dy}{dt} = \pm \sqrt{\frac{-2g \left[y \left(\frac{y^2}{6} + \frac{y_A y}{4} - y_A^2 \right) - \frac{v_F^2 y_A^2}{2g} \right]}{\left(\frac{y}{2} + y_A \right)^2}} \quad (\text{C-27})$$

$$\Rightarrow \int_0^t dt = t = \pm \int_0^y \frac{1}{\sqrt{\frac{-2g \left[y \left(\frac{y^2}{6} + \frac{y_A y}{4} - y_A^2 \right) - \frac{v_F^2 y_A^2}{2g} \right]}{\left(\frac{y}{2} + y_A \right)^2}} dy \quad (\text{C-28})$$

D Deceleration System Data Collection

Using a Canon Powershot A260 camera, this series of tests were conducted and recorded. Using these recordings, the nearly instantaneous position of the dummy load was determined. The video technique utilized the white wall near the experiment site. Before analysis of every video, each video frame was subtracted from the background. Since the object was black, this step resulted in a white object against a dark background. In addition, all stationary objects were eliminated in this process and only moving objects remained. Other moving objects were the ropes and the chain which did not have as much contrast as the falling object against the white wall. By carefully adjusting the threshold, all pixels except the one on the falling object can be eliminated. Next, the pixels in the image are summed up horizontally, which gave a peak at the location of the dummy load in every frame. The middle of the peak is the location of the dummy load.

The set up for the camera is shown in Figure 1. The camera was always kept at a constant distance 'D' away from the line of drop. The height of the camera was also maintained at 'H' in all experiments. The total distance that could be measured with this setup was around 11ft. D was equal to 143 inches and H was 53 inches. The greater D is, the more accurate the linear conversion factor becomes because of small angle approximation. However, an extremely large D can result in loss of accuracy since the pixel to distance ratio becomes larger. The perfect distance is when the camera is closest to the line of drop and can also capture the entire drop. A marker was placed on the wall and all distances were computed with reference to the marker then converted to distance from the reference line (horizontal line perpendicular from the camera to the wall). This process ensured that small movements of the camera did not alter the relative distance between the reference line and the object.

Since 12 ft of drop height was converted to 640 pixels, the conversion factor is about 0.225 inches/pixel. A more accurate conversion factor was calculated by placing a tape measure along the line of drop of the object, and taking a snapshot of the tape measure. By measuring the distance between the markings on the inch tape measure in pixels and plotting a graph of distance in inches versus distance in pixels, a conversion factor can be calculated. The conversion factor was 0.2182 inches/pixels. The standard deviation of error imposed by using this linear conversion factor was 0.2464 inches and the maximum error was 0.71. The source of the error in conversion factors is the simple assumption that the conversion factor is constant. The conversion factor is not constant because distances above the reference line appear smaller than they actually are, as the camera captures it from an angle. Using trigonometry or by experimentation, a more accurate variable conversion factor could have been derived. However, the uncertainties involved in using a constant conversion factor were negligible compared to accuracy gained.

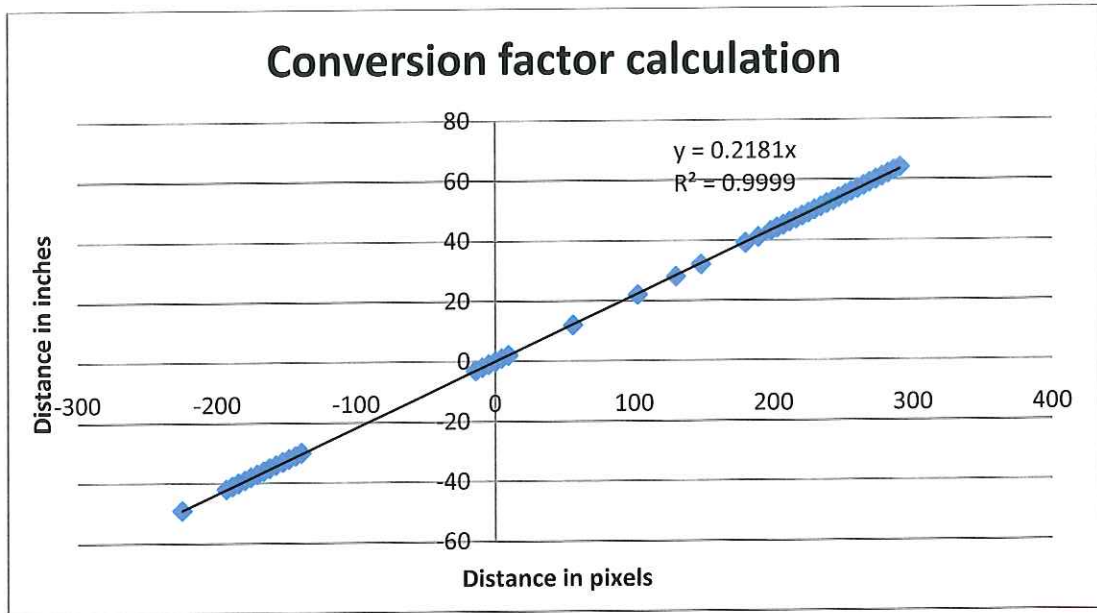


Figure D-1: Plot of actual distance versus pixels distance used to derive a conversion factor.

E Specifications

E.1 Efika MX Specifications^[10]

Freescale i.MX515 (ARM Cortex-A8 800MHz)
3D Graphics Processing Unit
WXGA display support (HDMI)
Multi-format HD video decoder and D1 video encoder
512MB RAM
4GB Internal SSD
802.11 b/g/n WiFi
Bluetooth
SDHC card reader
2x USB 2.0 ports
Audio jacks for headset
Built-in speaker



Figure E-1: Efika MX Microcomputer

E.2 Efika 5200B Specifications

Freescale MPC5200B System-on-Chip up to 400MHz

118mm x 153mm x 38mm

128MB 266MHz DDR RAM

44-pin IDE connector

10/100Mbit/s Ethernet

2x USB ports

1x RS232 Serial port

Stereo Audio out, Microphone and Line-input

33/66MHz PCI with bundled 90° AGP riser slot

RoHS Compliant



Figure E-2: Efika5200B Microcomputer

E.3 Camera Specifications^[7]

USB2.0 Global Shutter 752x480 8bit Mono CMOS Cameras with 32MB On-Board Memory

(Models: BCN-BG04-U, BCN-BG04-US, BCE-BG04-U and BCE-BG04-US)

PRODUCT DESCRIPTION

FEATURES

- ◆ Built-in frame buffer (23 frames at full resolution)
- ◆ True Global Shutter
- ◆ Support simultaneous image capturing from multiple cameras
- ◆ 4-pin GPIOs
- ◆ 752x480 active imaging pixels
- ◆ Arbitrary ROI supported
- ◆ Ultra compact
- ◆ High-speed USB2.0 (480Mb/s)
- ◆ Digital output, no need for frame grabber
- ◆ Custom programmable with SDK provided
- ◆ TWAIN driver
- ◆ USB command set protocol for non-Windows-based applications
- ◆ External and software trigger
- ◆ Strobe output for external flash
- ◆ Precise Frame Rate Setting
- ◆ Pixel skipping/binning
- ◆ No need for external power supply
- ◆ OEM versions available

APPLICATIONS

- ◆ Machine vision
- ◆ Digital microscopy
- ◆ Medical imaging
- ◆ Semiconductor equipment
- ◆ Test instruments
- ◆ High-quality ID photo capture
- ◆ Document scanners
- ◆ 2D barcode readers
- ◆ Web camera and security video

Mightex USB 2.0 cameras with frame buffers and global shutter are optimized for machine-vision applications, and they can also be used for a wide variety of other applications such as digital microscopy and medical imaging, where quality, ease of use, and cost-effectiveness are crucial. These cameras have built-in frame buffers, global shutter, external trigger-in, strobe-out, and a powerful camera engine that supports multiple cameras. Frame rate can be as high as 60 fps in full resolution and up to 600 fps using ROI mode. In addition, a user-friendly GUI based application software and an SDK are provided for custom software development. A USB command set protocol is also provided for non-Windows based applications.



PERFORMANCE SPECIFICATIONS

Parameters	BCN-BG04-U (C-mount) BCN-BG04-US (CS-mount)	BCE-BG04-U (C-mount) BCE-BG04-US (CS-mount)	Unit
Board-level/enclosed	Board-level	Enclosed	
Number of GPIOs	4	4	
Resolution	752x480 Monochrome		
CMOS Chip	1/3" Micron MT9V032, global shutter (Micron TrueSNAP)		
Pixel Size	6.0x6.0		μm
Scanning System	Progressive		
Dynamic Range	>55		dB
Gray Level	8		bit
Responsivity	4.8		V/lux-sec
On-board Memory ("Frame Buffers")	32		MB
Frame Rates* (@26MHz Clock)	60 @752x480 65 @640x480 130 @320x240 220 @160x120 310 @64 x 64		fps
Sub Resolutions* ¹	Support arbitrary ROI (Nx, Ny), with Nx and Ny multiples of 4		
Shutter Speed (Exposure time)	0.05~750		ms
Hardware Gains	1X - 4X		
Trigger Mode	With external trigger		
Strobe Out	Yes		
Lens mount	C-mount or CS-mount (M12.5-mount or custom-defined lens mount supported)		
Built-In Filters	No filter (standard), IR-cut, or IR-pass		
Power consumption	< 1.8		W
Dimension	51 x 51 x 29 (CS-mount) 51 x 51 x 34 (C-mount)	58 x 58 x 34 (CS-mount) 58 x 58 x 39 (C-mount)	mm
Weight (excluding lens)	80	150	g

* The actual achievable frame rate depends on exposure time, as well as resources available from the PC system.

E.4 Lens Specifications^[7]

H0514-MP

5mm F1.4

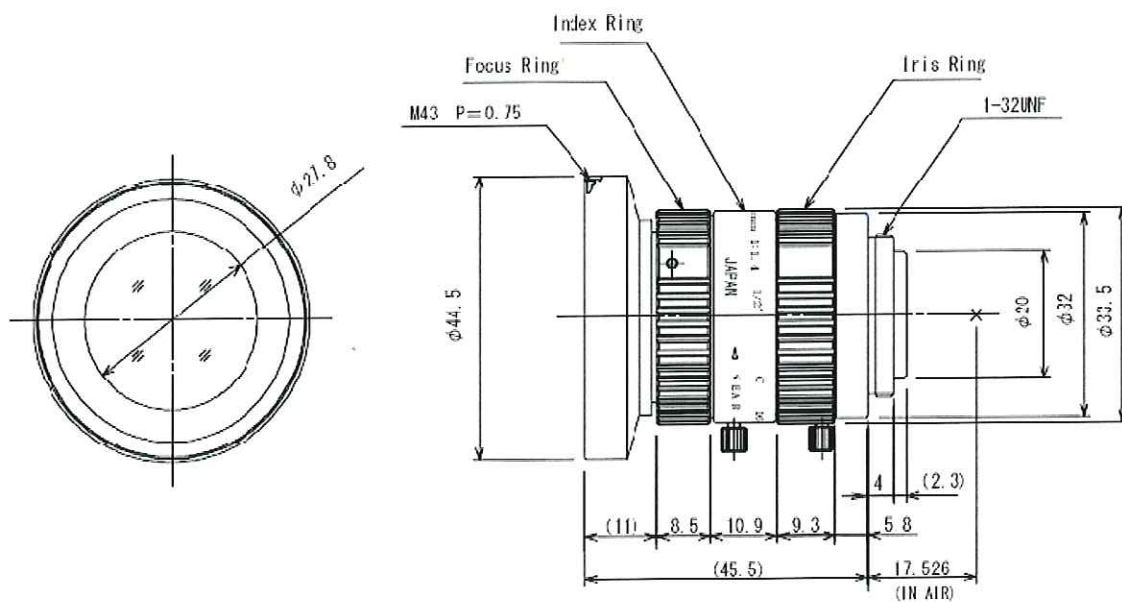
for 1/2 type Megapixel Cameras

C-Mount

Model No		H0514-MP		Effective	Front	φ 27.8mm	
Focal Length		5mm		Lens Aperture	Rear	φ 14.8mm	
Max. Aperture Ratio		1:1.4		Back Focal Length		10.8mm	
Max. Image Format		6.4mm x 4.8mm(φ 8mm)		Flange Back Length		17.526mm	
Operation Range Object Dimension at M.O.D	Iris	F1.4~16C		Mount		C-Mount	
	Focus	0.1m~Inf. 12.9 x 9.6cm		Filter Size Dimensions		M43 P=0.75 φ 44.5mm X 45.5mm	
				Weight		107 g	
Angle of View	D	1/2 type	76.7°	1/3 type	62.3°	1/4 type	48.5°
	H		65.5°		51.4°		39.5°
	V		51.4°		39.5°		30.0°
Operating Temperature		-20℃ - +50℃					

M.O.D : Minimum Object Distance

Dimensions



E.5 Circuit Board Relay Specifications

tyco
Electronics

Catalog 1308242
Issued 3-03

P&B



Features

- Up to 30A switching in SPST and 20A switching in SPDT arrangements.
- Silver cadmium oxide contacts.
- Available as an open frame relay, with a snap-on dust cover or with an immersion cleanable⁽²⁾, plastic sealed case.
- Meets UL 508 & UL 873 spacing - 1/8" through air, 1/8" over surface (1/4" over surface with terminal code 4)
- UL class F insulation standard.
- Well suited for various industrial, commercial and residential applications, as well as many others.

Contact Ratings @ 25°C

Arrangements: 1 Form A (SPST-NO) and 1 Form C (SPDT).

Material: Silver cadmium oxide.

Mechanical Life: 10 million operations, typical.

Contact Ratings @ 25°C with relay properly vented. Remove vent nib after soldering and cleaning.

Typical Electrical Load & Life (Open Style Relay)

Form & Contact Material	Contact Load	Type of Load	Ops
(1) Silver cadmium oxide	30A @ 240VAC	UL General Purpose	100,000
	20A @ 240VAC	Resistive Heater	100,000
(5) Silver cadmium oxide	20A/10A @ 240VAC	UL General Purpose	100,000
	20A/10A @ 28VDC	Resistive	100,000

Minimum Contact Load:

Silver Contacts: 500mA @ 5VDC or 12VAC.

Silver Cadmium Oxide Contacts: 1A @ 5VDC or 12VAC.

Initial Contact Resistance: 75 mΩ, max., @ min. rated current (switched).

Initial Dielectric Strength

Between Open Contacts: 1,500V rms.

Between Contacts and Coil: 1,500V rms (terminal code 1).

2,500V rms (UL 873 version terminal code 4).

Initial Insulation Resistance

Between Mutually Insulated Elements: 10⁹ ohms, min., @ 500VDC, 25°C and 50% R.H.

Coil Data @ 25°C

Voltage: 5 to 110VDC.

Maximum Coil Power: 2.8 Watt

Maximum Coil Temperature⁽⁵⁾: Class F: 155°C.

Duty Cycle: Continuous.

Coil Data

Nominal Voltage (VDC)	Resistance ± 10% (Ohms)	Nominal Power (mW)	Nominal Current (mA)
5	27	930	185
6	40	900	150
9	97	840	93
12	155	930	77
15	256	880	59
18	380	850	47
24	660	870	36
48	2,560	900	19
110	13,450	900	8

Operate Data @ 25°C

Must Operate Voltage: 75% of nominal voltage or less.

Must Release Voltage: 10% of nominal voltage or more.

Operate Time (Including Bounce): 15 ms, max.

Release Time (Including Bounce): 15 ms, max.

1 At or from Nominal Coil Voltage

T90 series

30 Amp Printed Circuit Board Relay

File E22575

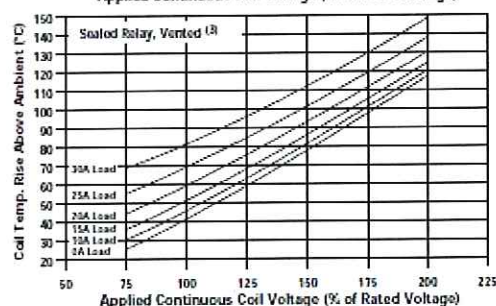
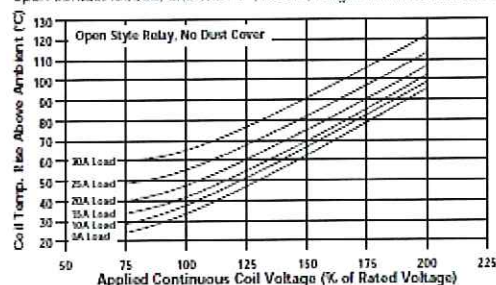
File LR15734

Patented

Users should thoroughly review the technical data before selecting a product part number. It is recommended that user also seek out the pertinent approvals files of the agencies/laboratories and review them to ensure the product meets the requirements for a given application.

Typical Coil Temperature Rise

Data below are average values and should be verified in application. Tests were conducted within a 2' (6 m) cube (still air) with relay mounted to a 30A, single side P.C. board⁽⁶⁾, at nominal coil power @ 25°C; with normally open contact loaded; and with 4' (1.22 m) long, #10 AWC load wires.



Environmental Data

Storage Temperature Range: -40°C to 130°C.

Operating Temperature Range: -55°C to +85°C(1).

Vibration, Operational: 0.065" (1.65mm) max. excursions from 10-55 Hz, with no contact opening > 100μs.

Shock, Operational: 10g for 11 ms with no contact opening > 100μs.

Shock, Mechanical: 100g.

Mechanical Data

Termination: Printed circuit terminals⁽⁴⁾.

Enclosures (all have 94V-0 flammability rating, Class F temp. rating):

Optional dust cover: Snap on plastic dust cover is available for use on open style T90N.

Sealed case (T90S): Immersion cleanable, sealed plastic case⁽²⁾.

Weight: Open Model T90N: 0.7 oz. (20g) approximately.

Sealed Model T90S: 0.9 oz. (26g) approximately.

Notes

- (1) Operating ambient temperature must consider "Must Operate Voltage Change Over Temperature," Contact Temperature Rise, Coil Temperature Rise (if coil is not allowed to cool) and Maximum Coil Temperature. Specification ambient considers nominal coil voltage, 20A load with coil cooled to ambient.
- (2) Sealed relay terminals should not be bent.
- (3) Knock off nib should be removed after cleaning process for optimum life of sealed relays.
- (4) Maximum soldering temperature is 500°F for 4 seconds.
- (5) Class F coils are UL systems approved for maximum coil temperature of 155°C by change of resistance method.
- (6) See application note 13C265 for proper relay mounting, termination, cleaning and PC board conductor width. Coil rise test performed with 30A PC board to maintain 20°C maximum rise @ 30A.

E.6 Darlington Array Specifications



Octal High Voltage, High Current Darlington Transistor Arrays

The eight NPN Darlington connected transistors in this family of arrays are ideally suited for interfacing between low logic level digital circuitry (such as TTL, CMOS or PMOS/NMOS) and the higher current/voltage requirements of lamps, relays, printer hammers or other similar loads for a broad range of computer, industrial, and consumer applications. All devices feature open-collector outputs and free wheeling clamp diodes for transient suppression.

The ULN2803 is designed to be compatible with standard TTL families while the ULN2804 is optimized for 6 to 15 volt high level CMOS or PMOS.

MAXIMUM RATINGS ($T_A = 25^\circ\text{C}$ and rating apply to any one device in the package, unless otherwise noted.)

Rating	Symbol	Value	Unit
Output Voltage	V_O	50	V
Input Voltage (Except ULN2801)	V_I	30	V
Collector Current – Continuous	I_C	500	mA
Base Current – Continuous	I_B	25	mA
Operating Ambient Temperature Range	T_A	0 to +70	$^\circ\text{C}$
Storage Temperature Range	T_{stg}	-55 to +150	$^\circ\text{C}$
Junction Temperature	T_J	125	$^\circ\text{C}$

$R_{\theta JA} = 55^\circ\text{C/W}$

Do not exceed maximum current limit per driver.

ORDERING INFORMATION

Device	Characteristics		
	Input Compatibility	$V_{CE}(\text{Max})/I_C(\text{Max})$	Operating Temperature Range
ULN2803A	TTL, 5.0 V CMOS	50 V/500 mA	$T_A = 0 \text{ to } +70^\circ\text{C}$
ULN2804A	6 to 15 V CMOS, PMOS		

Order this document by ULN2803/D

**ULN2803
ULN2804**

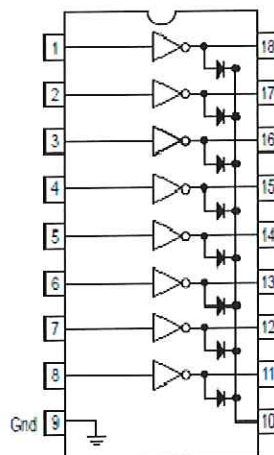
**OCTAL PERIPHERAL
DRIVER ARRAYS**

**SEMICONDUCTOR
TECHNICAL DATA**

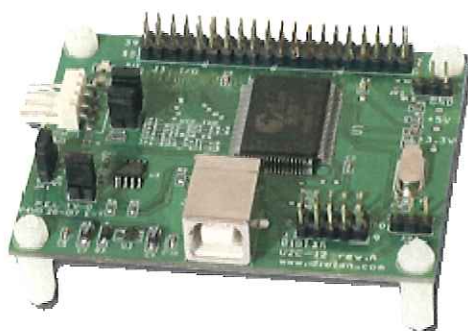


**A SUFFIX
PLASTIC PACKAGE
CASE 707**

PIN CONNECTIONS



E.7 USB - I2C/SPI/GPIO Adapter - U2C-12 Specifications



- USB to I2C interface with configurable I2C clock frequency up to 400kBit/s.
- USB to SPI interface with configurable phase, polarity and frequency.
- Up to 23 user configurable GPIO.
- Fast and easy In-Circuit Programming (ICP) of different I2C EEPROMs, SPI EEPROMs and in-circuit programming capable microcontrollers like Atmel AVR
- Wide range of ready to use applications with free source code.
- Linux/Windows/MacOS C, C++, VB, VB.net sample code.
- Flexible and powerful API for custom software development in Windows, Linux and MacOS environment.

General Description

- Diolan U2C-12, all-in-one SPI-USB, I2C-USB and GPIO-USB Adapter provides a low cost solution to connect your PC to I2C and SPI slave devices.
- U2C-12 Adapter drivers, libraries and software turns your PC running Windows, Linux or MacOS into a comprehensive I2C and SPI master device. You can also use our API to integrate U2C-12 Adapter with your own software. All you need is to link your software with U2C-12 library and call its functions.
- U2C-12 Adapter I2C module has very flexible I2C interface. You can configure I2C frequency, send high level I2C transactions, low-level I2C commands or work directly with I2C lines. See our article about I2C interface for more details.
- U2C-12 Adapter SPI module supports all 4 SPI modes, which are configured using CPOL and CPHA parameters. You can connect up to 20 different SPI slave devices to

single USB-I2C/SPI Interface Adapter. See our article about SPI interface for more details.

- Up to 128 U2C-12 Adapters can be simultaneously connected to one PC. Each adapter has unique serial number that can be used to identify it on the USB bus.
- <http://www.diolan.com/i2c/u2c12.html>

F West Brook Metals Information Sheet

Phone: (210)-661-4146

Address: 410 South and I-10

Table F-1: Housing Size and Cost Estimate

			sides, x4	ends, x2					
l, in	36.63	surface area (in ²)	1030	791		Grade	14	16	18
w, in	28.13					Thickness (in)	0.032	0.04	0.05
h, in	28.13					Unit Weight (lbs/ft ²)	0.474	0.593	0.741
		Total Surface Area (in ²)	5702			Unit Cost	\$1.56	\$2.00	\$2.45
		Total Surface Area (ft ²)	40						
						Total Weight (lbs/ft ²)	18.7702 1	23.4825 7	29.3433 1
						Total Cost	\$61.78	\$79.20	\$97.02

G Test Matrix

Dummy Weight	Chain Amount (Lengths)	Free Fall Displacement		
		3 Feet	6 Feet	9 Feet
5 pounds	1	<i>Resolution low on first two of four runs</i>	<i>Final height: 105 in, 107 ½ in</i>	—
	2		<i>Final height: 8 ft, 8 ft</i>	
	3		<i>Final height: 91 in, 93 ½ in</i>	<i>Final height: 124 ½ in</i>
10 pounds	1			—
	2			—
	3			
	4	—		
	5	—	—	<i>Final height: 124 ½ in</i>
15 pounds	1		—	—
	2			—
	3		<i>Final height: 119 in</i>	—
	4		<i>Final height: 105 in</i>	—
	5	—	—	
	6	—	—	
20 pounds	1		—	—
	2		—	—
	3			—
	4			—
	5			—
	6	—	—	
	7	—	—	

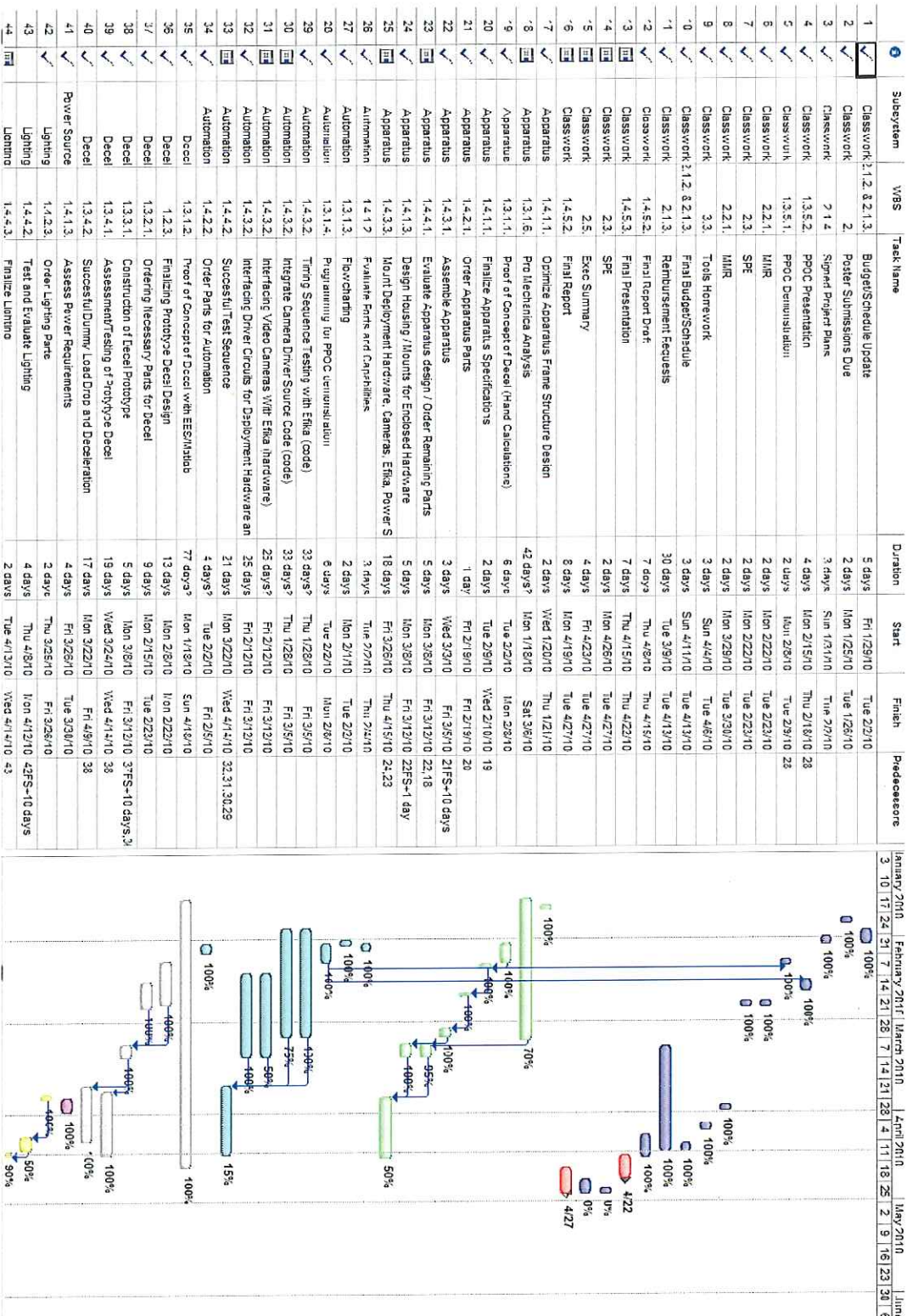
H Bill of Materials and Vendor List

Table H-1: Bill of Materials and Vendor List

Date	Vendor	Part Number	Item Description	Quantity	Price/Ea	Actual Amount
11/18/2009	Mevicon	NT03-641	Benchplate, 36" x 4"	1	\$215	\$215.00
12/8/2009	Genesi USA		Efika MX microcomputer	1	\$249	\$249.00
2/8/2010	Mightex	BCE-BG04-U	Wide VGA 752x480 Monochrome 8-bit CMOS Camera	2	\$459.00	\$918.00
2/8/2010	Mightex	M0814-MP	Lens for camera level with shell	1	\$161.00	\$161.00
2/8/2010	Mightex	M0814-MP	Lens for camera directly above shell	1	\$161.00	\$161.00
2/11/2010	Womack	3842535571	10 mm inside-to-inside gusset and set screws	4	\$5.20	\$20.80
2/11/2010	Womack	3842529397	40 mm corner cube kit 3S	8	\$10.92	\$87.36
2/11/2010	Womack	1522411	849MM profile 40x40	4	\$25.75	\$103.00
2/11/2010	Womack	1522412	635MM profile 40x40	10	\$20.08	\$200.80
2/11/2010	Womack	8981021323	10mm T-Nuts with 1/4"x20 UNC	4	\$0.94	\$3.76
3/6/2010	Ozium		Silicone Encased LED Strips - Warm White	3	\$14.99	\$44.97
3/8/2010	Newegg.com	12-270-112	CABLE BYTECC HDMID-3 R	1	\$5.49	\$5.49
3/24/2010	Intertex	UB1250	12V Battery	1	\$14.95	\$14.95
4/7/2010	Womack	8981021323	10mm T-Nuts with 1/4"x20 UNC	72	\$0.94	\$67.68
4/7/2010	Womack	3842532235	40x40 multi-angle connector kit	2	\$35.98	\$71.96

4/7/2010	Womack	3842535571	10 mm inside-to-inside	3	\$5.20	\$15.60
gusset and set screws						
4/7/2010	Womack	8981021468	T Head Bolt	2	\$1.38	\$2.76
4/7/2010	Womack	3842993120	635MM profile 40x40	1	\$22.18	\$22.18
Total Expenses						\$2,365.31

I Schedule



J Budget

Table J-1: Project Income

Income						
Date	Sponsor	Description		Status	Budgeted Amount	Actual Amount
9/1/2009	Engr Dept	Senior Design Project Allotment		Received	\$1,200.00	\$1,200.00
11/13/2009	IEEE CTS	Phase II IEEE student branch funding		Received	\$1,000.00	\$985.34
11/18/2009	Mevicon	Benchplate, 36" x 4"		Received	\$215.00	\$215.00
12/8/2009	Genesi USA	Efika MX microcomputer		Received	\$249.00	\$249.00
3/12/2010	Engr Dept	Additional Allocation		Received	\$375.00	\$375.00
				Total	\$3,039.00	\$3,024.34

Table J-2: Project Expenses

Expenses					
Date	Vendor	Item Description	Quantity	Budgeted Amount	Actual Amount
11/18/2009	Mevicon	Benchplate, 36" x 4"	1	\$215.00	\$215.00
12/8/2009	Genesi USA	Efika MX microcomputer	1	\$249.00	\$249.00
2/8/2010	Mightex	Wide VGA 752x480 Monochrome 8-bit CMOS Camera	2	\$918.00	\$918.00
2/8/2010	Mightex	Lens for camera level with shell	1	\$161.00	\$161.00
2/8/2010	Mightex	Lens for camera directly above shell	1	\$161.00	\$161.00
				\$43.00	\$43.00
2/11/2010	Womack	10 mm inside-to-inside gusset and set screws	4	\$20.80	\$20.80
2/11/2010	Womack	40 mm corner cube kit 3S	8	\$87.36	\$87.36
2/11/2010	Womack	849MM profile 40x40	4	\$103.00	\$103.00
2/11/2010	Womack	635MM profile 40x40	10	\$200.80	\$200.80
2/11/2010	Womack	10mm T-Nuts with 1/4"x20 UNC	4	\$3.76	\$3.76
				\$47.69	\$47.69

2/26/2010	Grainger	cable, 1/4 In, L 50ft, WLL 1400Lb, 7x19	1	\$52.34	\$52.34
2/26/2010	Grainger	Clip, Wire Rope, 1/4 In Wire Rope Dia	4	\$15.96	\$15.96
2/26/2010	Grainger	Chain, Steel, Grade 30, 1/2 In, 20 Ft	1	\$101.39	\$101.39
2/26/2010	Grainger	Chain, Steel, Grade 30, 1/2 In, 50 Ft	1	\$237.60	\$237.60
2/26/2010	Grainger	Pulley, Heavy Duty, Flat Mount, 5/16 In	2	Product returned	Product returned
3/6/2010	Ozium	Silicone Encased LED Strips - Warm White	3	\$44.97	\$44.97
				\$4.20	\$4.20
3/4/2010	Newegg.com	CABLE BYTECC HDMID-3 R	1	\$5.49	\$5.49
				\$2.99	\$2.99
3/10/2010	Home Depot	Spring Lock	1	\$3.79	\$3.79
3/10/2010	Home Depot	Torx Head Driver Pkg	1	\$14.97	\$14.97
				\$1.52	\$1.52
3/10/2010	Home Depot	Washers	4	\$0.52	\$0.52
3/10/2010	Home Depot	Washers	4	\$0.96	\$0.96
3/10/2010	Home Depot	Hex Nuts	4	\$0.44	\$0.44
3/10/2010	Home Depot	Hex Bolt	4	\$3.60	\$3.60
				\$0.45	\$0.45
3/24/2010	Intertex	12V Battery	1	\$14.95	\$14.95
3/24/2010	Intertex	PBC Relay	1	\$2.95	\$2.95
				\$1.45	\$1.45
3/29/2010	Grainger	Rope Load Block, Loop Top, WLL880Lb	2	\$33.04	\$39.52

4/7/2010	Womack	10mm T-Nuts with 1/4"x20 UNC	72	\$67.68	\$67.68
4/7/2010	Womack	40x40 multi-angle connector kit	2	\$71.96	\$71.96
4/7/2010	Womack	10 mm inside-to-inside gusset and set screws	3	\$15.60	\$15.60
4/7/2010	Womack	T Head Bolt	2	\$2.76	\$2.76
4/7/2010	Womack	635MM profile 40x40	1	\$22.18	\$22.18
				\$20.92	\$20.92
4/14/2010	Altex	USB2.0 4 way splitter	1	\$7.52	\$7.52
4/26/2010		Final Report Binding	1	\$15.00	
				\$2,977.61	\$2,969.09
				Budgeted	Actual
				\$61.39	\$55.25